Front. Mech. Eng. 2022, 17(2): 24
https://doi.org/10.1007/s11465-022-0680-8

REVIEW ARTICLE

Fiber-reinforced composites in milling and grinding: machining bottlenecks and advanced strategies

Teng GAO[a], Yanbin ZHANG[a], Changhe LI (✉)[a], Yiqi WANG[b], Yun CHEN[c], Qinglong AN[d], Song ZHANG[e], Hao Nan LI[f], Huajun CAO[g], Hafiz Muhammad ALI[h], Zongming ZHOU[i], Shubham SHARMA[j]

[a] *School of Mechanical and Automotive Engineering, Qingdao University of Technology, Qingdao 266520, China*
[b] *School of Mechanical Engineering, Dalian University of Technology, Dalian 116024, China*
[c] *Chengdu Tool Research Institute Co., Ltd., Chengdu 610500, China*
[d] *School of Mechanical Engineering, Shanghai Jiao Tong University, Shanghai 200240, China*
[e] *School of Mechanical Engineering, Shandong University, Jinan 250061, China*
[f] *School of Aerospace, University of Nottingham Ningbo China, Ningbo 315100, China*
[g] *School of Mechanical Engineering, Chongqing University, Chongqing 400044, China*
[h] *Mechanical Engineering Department, King Fahd University of Petroleum and Minerals, Dhahran 31261, Saudi Arabia*
[i] *Hanergy (Qingdao) Lubrication Technology Co., Ltd., Qingdao 266100, China*
[j] *Department of Mechanical Engineering, IK Gujral Punjab Technical University, Punjab 144603, India*

✉ *Corresponding author. E-mail: sy_lichanghe@163.com (Changhe LI)*

ABSTRACT Fiber-reinforced composites have become the preferred material in the fields of aviation and aerospace because of their high-strength performance in unit weight. The composite components are manufactured by near net-shape and only require finishing operations to achieve final dimensional and assembly tolerances. Milling and grinding arise as the preferred choices because of their precision processing. Nevertheless, given their laminated, anisotropic, and heterogeneous nature, these materials are considered difficult-to-machine. As undesirable results and challenging breakthroughs, the surface damage and integrity of these materials is a research hotspot with important engineering significance. This review summarizes an up-to-date progress of the damage formation mechanisms and suppression strategies in milling and grinding for the fiber-reinforced composites reported in the literature. First, the formation mechanisms of milling damage, including delamination, burr, and tear, are analyzed. Second, the grinding mechanisms, covering material removal mechanism, thermal mechanical behavior, surface integrity, and damage, are discussed. Third, suppression strategies are reviewed systematically from the aspects of advanced cutting tools and technologies, including ultrasonic vibration-assisted machining, cryogenic cooling, minimum quantity lubrication (MQL), and tool optimization design. Ultrasonic vibration shows the greatest advantage of restraining machining force, which can be reduced by approximately 60% compared with conventional machining. Cryogenic cooling is the most effective method to reduce temperature with a maximum reduction of approximately 60%. MQL shows its advantages in terms of reducing friction coefficient, force, temperature, and tool wear. Finally, research gaps and future exploration directions are prospected, giving researchers opportunity to deepen specific aspects and explore new area for achieving high precision surface machining of fiber-reinforced composites.

KEYWORDS milling, grinding, fiber-reinforced composites, damage formation mechanism, delamination, material removal mechanism, surface integrity, minimum quantity lubrication

1 Introduction

Fiber-reinforced composites can reduce the weight of components greatly because of their high specific strength and stiffness [1,2]. Moreover, these materials can carry out the integrated design and manufacturing of material structure and function, which easily realizes the overall manufacturing of large and complex components to reduce the connection greatly [3]. Therefore, fiber-reinforced composites have become the preferred

Received November 7, 2021; accepted February 14, 2022

materials for aerospace equipment, such as rocket nose cone and fairing shell. In addition, fiber composites with special structure have been successfully applied to the nuclear reactor cooling system of nuclear submarine because of its vibration and noise reduction capabilities, as well as excellent high-temperature resistance. Ceramic matrix composites (CMCs) have been the preferred choice as replacement of more conventional materials in high-temperature applications for innovative industries, for instance, the replacement of nickel superalloys in aeroengines (pass duct case and seal adjusting plate) and aircraft brakes in the aerospace production and shielding for nuclear energy reactors. Fiber composites have been widely used in important scientific, technological, and military fields. Composites are manufactured by near net-shape by laying and curing, and there is also some 3D printing manufacturing at present [4,5]. However, to ensure the component accuracy and assembly requirements, the cured composite parts still need a lot of subsequent secondary processing of edge contour, functional window, and connecting hole [6].

The components of fiber-reinforced composite generally have large size and thickness, resulting in a large amount of material removal. The main processing method is still the machining of cutting, such as turning [7,8], milling [9,10], drilling [11,12], and grinding [13,14]. At present, the research on the drilling of fiber composites has been comprehensive, and a large number of reviews systematically analyzed and summarized the drilling damage mechanism and suppression strategies. However, in addition to drilling, milling and grinding are two indispensable and irreplaceable machining methods to ensure integrity [15]. Milling and grinding have similar and unique tool workpiece interference mechanisms [16,17]. Intermittent cutting refers to the removal of material by the cutting edge in milling [18,19]. In fact, grinding is also intermittent cutting microscopically, because of the random distribution of grains [20,21]. However, the scale of intermittent cutting varies [22]. Therefore, the defects produced by these two machining methods also have uniqueness and commonalities. One advantage of near net-shape manufacturing is that the final dimension and assembly tolerance can be achieved only by finishing machining, such as milling and grinding [23]. The boarding gate and porthole assembly port on the barrel structure of B787 integral fuselage must be milled [24]. Precision parts and mating locating surfaces shall be machined by precision grinding [25,26].

However, fiber-reinforced composites are heterogeneous from mesoscopic, which are composed of fiber, resin, and interface. Macroscopically, it has multi-layer and multi-directional heterogeneous anisotropy characteristics, with high hardness, anisotropy, lamination, and other characteristics. These composites are typical difficult-to-machine materials [27]. The problems related to composites (i.e., anisotropy and heterogeneity of composition) and the inherent brittleness of ceramic components and their interfaces complicate the study of the basic mechanism of abrasive removal process [28]. In addition, these problems combine the inherent randomness of the grinding process. Fiber or matrix fracture occurs very easily in the process of cutting, thereby resulting in quality defects, such as delamination, burrs, and cracks on the machined surface, wherein achieving the required machining accuracy and surface quality is difficult. It also leads to low tool life and frequent tool change, which causes difficulty in realizing high precision and digital machining [29]. The scrapping of components causes significant economic losses and even catastrophic accidents. Therefore, the high-quality and high-efficiency machining of fiber composite parts poses a severe challenge to existing cutting theory and technology.

In light of the above, the main objective of the present work is to provide a comprehensive review on the milling and grinding of fiber composite laminates. Therefore, this paper reviews the advances in milling damage formation, grinding mechanism, and suppression strategies systematically and comprehensively. The logical relationship of integral structure is shown in Fig. 1 [13,30,31]. Initially, the mechanism of material removal, delamination, burr, and tear in milling is analyzed. The evolution relationship among different damage forms is discussed. Subsequently, the grinding mechanisms, including material removal mechanism, thermal and mechanical behavior, surface integrity, and damage, are discussed microcosmically and macroscopically. Afterward, the suppression strategies available in the literature, including ultrasonic vibration assisted machining, cryogenic cooling, minimum quantity lubrication (MQL), tool geometry, and coatings, are summarized. Finally, conclusions, research gaps, and outlook are made, giving the researchers the opportunity to deepen specific aspects and explore new area for reaching high-precision surface machining of fiber-reinforced composites.

2 Milling damage formation mechanism

2.1 Material removal mechanism

The study of material removal mechanism in the cutting process plays a key role in the basic understanding of processing quality and damage formation. However, investigating the material removal mechanism is often difficult because of the heterogeneity and obvious anisotropy of fiber-reinforced composites. Various types of fiber-reinforced materials and their structures also limit any conclusive or generalized theory related to the chip formation of these composites. The material removal mechanism of milling in different fiber directions is diverse because of the anisotropy of fiber composites.

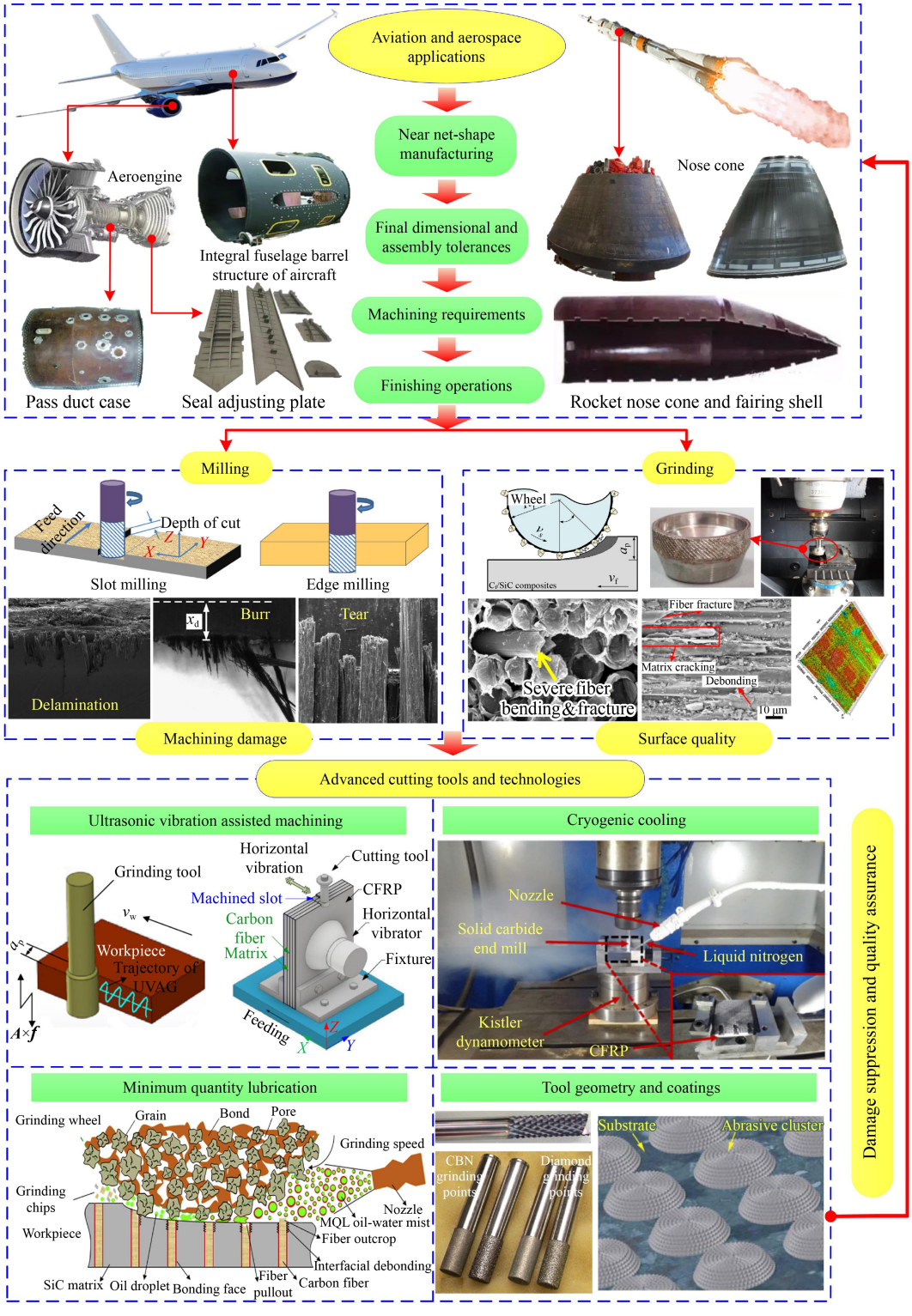

Fig. 1 Logical relationship of integral structure. Reproduced with permission from Refs. [13,30,31] from Elsevier.

Koplev et al. [32] conducted an experimental comparison of cutting unidirectional carbon fiber-reinforced plastic (UD-CFRP) perpendicular and parallel to the fiber direction using a fast stop device. Poor surface quality and serious sub surface tear are produced when cutting perpendicular to the fiber direction. The machined surface parallel to the fiber direction is smooth. To understand the cutting behavior of carbon fiber-reinforced plastic (CFRP) more intuitively, Kaneeda and Takahashi [33] observed the formation of CFRP chips online by using a scanning electron microscope. In unidirectional fiber reinforced polymer (FRP) chips, chip formation is highly

dependent on fiber orientation [34]. The size of discontinuous chips decreases with the increase in fiber orientation at 0° < fiber cutting angle (FCA) < 45°. No significant change in chip formation was observed when FCA > 45°. In the trimming process in the direction of 0°–90° fibers, the fracture plane in which the chip release occurred was parallel to the fiber direction along the fiber-matrix interface. Three different cutting mechanisms can be used in the unidirectional FRP trimming. In the 0° fiber orientation, the chip formation mechanism includes cantilever bending failure along the fiber matrix interface and fracture perpendicular to the fiber direction. In the case of 75° fiber orientation, chip formation involves compressive load induced shear at the tool tip. When FCA > 90°, chip formation and material removal include out-of-plane shear and in-layer deformation caused by severe compressive load. Nayak et al. [35] found that the chip length and broken fiber length of the CFRP milling decreased with the increase in fiber orientation. Tensile fracture is the main cause of fiber fracture when FCA > 90°. Li et al. [36] showed that chips are produced by matrix fiber interface shear along the fiber direction at 15° < θ < 75°. When the fiber angle exceeds 75°, the chip will yield because of the bending fracture, and the fiber may rebound in the cutting process to reduce the surface roughness of the machined surface. According to the fiber direction and the rake angle of the cutting edge, the chip formation of CFRP unidirectional plate can be divided into five types [37,38]. For the 0° fiber direction, the chip formation mode includes delamination type and fiber buckling type. It is shown as cracking along the fiber/resin interface and fracture perpendicular to the fiber direction under bending load. When 0° < FCA < 90°, regardless of the positive and negative rake angles, the chip formation mode is fiber cut-off, which is manifested as the shear fracture caused by extrusion at the fiber cross section and inter-laminar shear fracture at the fiber/resin interface. Chip flow is formed in a plane parallel to the fiber direction. The tool movement causes serious fiber deformation when the FCA > 90°, thereby resulting in delamination and shear at the fiber/resin interface. Li et al. [36] divided the energy consumption in CFRP processing into three parts: new surface energy, friction energy, and chip fracture energy. The chip friction energy is dominant, followed by new surface energy and chip fracture energy. The energy consumption of newly machined surfaces decreases with the increase in FCA. The milling force of 45°/135° fiber direction laminate is smaller than that of 0°/90° fiber direction laminate. The location of the maximum tangential force is matched with the area generated by delamination [39]. Machining surface damage mainly includes hole defects caused by local single carbon fiber fracture, surface cracks caused by elastic bending deformation of carbon fiber, and voids or incomplete adhesion between carbon fiber and matrix. Two types of carbon fiber fracture can be observed during processing: shear fracture and bending fracture. Open or tear cracks also exist in the matrix, and the deformation of the fiber will also lead to the breakage of the matrix. In addition, open and sliding cracks are seen at the interface [40]. Ghafarizadeh et al. [41] believed that the propagation of processing damage was also closely related to fiber orientation. In the milling process with machining direction of 0°, the compression damage of uncut materials expands to the fiber direction. For 45° and 60° tool rotation, this failure mode will affect a large area of uncut material, and matrix cracking failure will also affect a relatively large area of uncut material below the tool. Discontinuous and broken chips are produced in the milling of glass fiber-reinforced plastics (GFRP) [42]. In the 45° and 90° fiber directions, the debris is crushed into powdery particles of fiber and epoxy resin matrix because of the out-of-plane fracture and extrusion of workpiece material by processing tools. The surface roughness of GFRP milling decreases with the increase in cutting speed and cutting depth and increases with the increment of feed rate [43]. The best surface quality can be obtained under low feed rate and high cutting speed [44]. For Kevlar 49 fiber composite, different fiber orientations will produce various forms of shear stress, which will lead to different forms of chip breaking, such as stretching or extrusion [45]. Moreover, acute angle cutting less than 45° has more advantages than obtuse angle cutting. At the same time, latitude fiber is responsible for increasing shear F_x and tensile F_y, and longitude fiber is responsible for extrusion F_x and shear F_y. When FCA = 30°, the lattice shear action is the largest, and then the shear action is weakened. Insufficient shear leads to residual burrs, but the longitude fiber is not affected.

2.2 Delamination

In the milling process, the cutting force will cause high inter-laminar stress in fiber composites. The high inter-laminar stress and low inter-laminar strength of fiber laminates will cause cracks between layers, and the cracks will gradually expand and cause delamination [46]. Delamination can be divided into interlayer and surface delamination. The surface layer of the fiber laminate is more prone to delamination than the interlayer because the surface fiber does not have enough supporting force provided by the matrix. Compared with unidirectional fiber composites, the interlayer effect caused by different fiber angles between the adjacent layers of multi-directional fiber composites has a greater impact on the material removal process, especially between layers with fiber angles of 90° and 135°. The main reason is that the interlayer effect of multi-directional laminates enhances the interlayer support provided by adjacent layers [47]. Figure 2 shows the

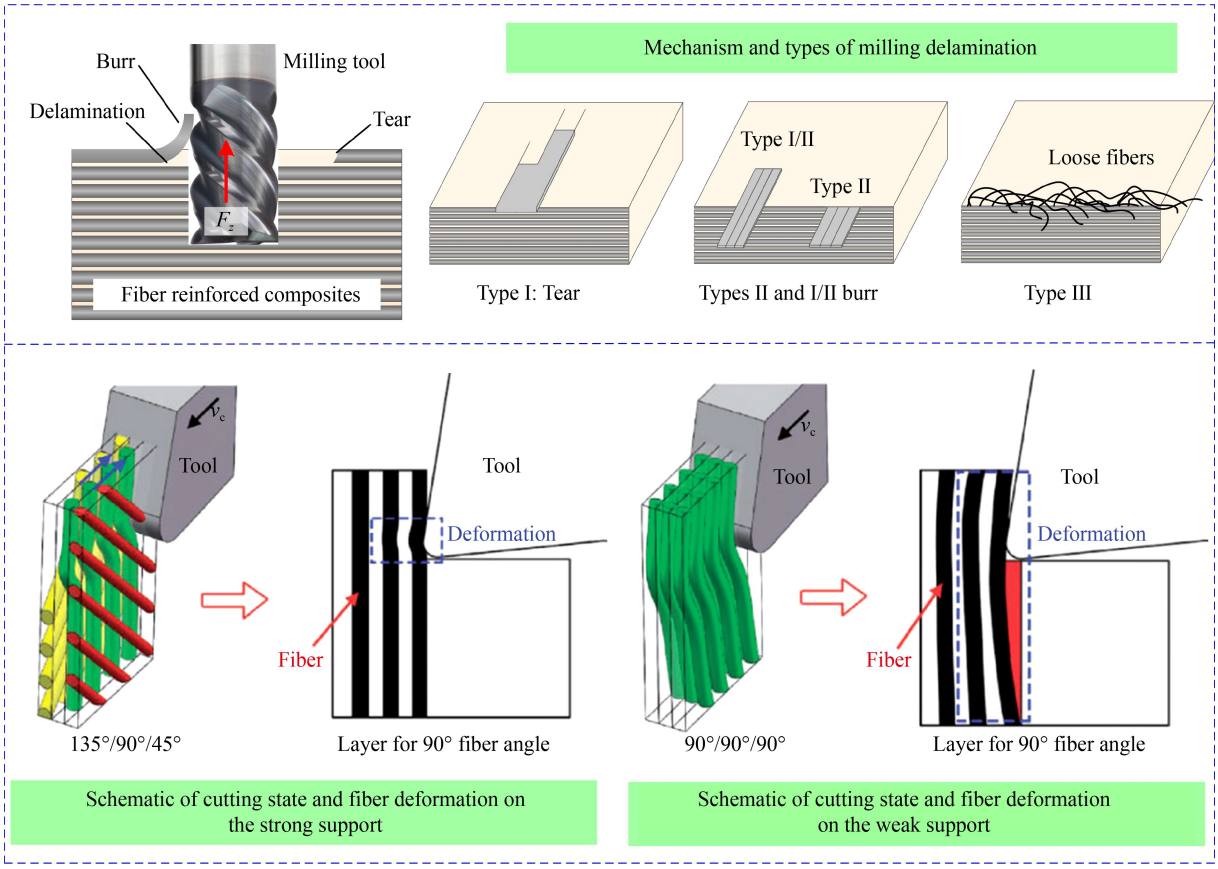

Fig. 2 Mechanism of milling delamination. Part of this figure was drawn based on Refs. [48,49] to introduce their comments. Reproduced with permission from Refs. [47] from SAGE Publications.

formation of surface delamination during milling [47–49]. In the milling process, the milling tool produces an axial milling force F_z on the workpiece because of the spiral angle. F_z has an upward pushing effect on the surface fiber. Delamination will occur when F_z is greater than the adhesion between the fiber and the matrix. F_z is the main cause of surface delamination; the cutting force first increases, then decreases, and finally increases with the FCA from 0° to 180° [50]. The cutting force increases with the feed rate and radial cutting depth [51]. Delamination directly affects the strength and fatigue resistance of composites. During milling, when the inter-laminar stress exceeds the inter-laminar and fiber bonding strength, debonding will occur between the fiber bundle and the matrix, accompanied by the deformation of the fiber layer. The deformation of the fiber layer would gradually recover after being cut. However, with the loss of the adhesion of the matrix, the delamination defect becomes permanent. Inter-laminar delamination may occur in any fiber layer of milling fracture [52]. Tears and burrs will show if it appears on the surface. Therefore, the delamination of the surface layer is the root cause of tearing and burr. Colligan and Ramulu [48] divided the surface delamination into three types (Fig. 2). The first type is that the fiber breaks along the axial direction and is pulled out from the matrix to form grooves and voids without fiber, that is, tear defects. The second type is that the fiber is not cut and hangs outward along the fiber direction, that is, burr defect. The third type is the presence of loose fibers along the feed direction at the milling edge. Sheikh-Ahmad et al. [53] proposed that the characteristics of delamination also included their types and occurrence frequencies. Delamination mainly occurs in the surface layer, and the delamination types are mainly types I/II and I. The average delamination depth rises with the increase in feed rate and the decrease in cutting speed, which corresponds to the increase in effective chip thickness. Colligan and Ramulu [48,49] attributed the delamination of fiber composite surface to the lack of support between the upper and lower layers. Hintze et al. [54] linked the FCA with delamination defects and found that the FCA tended exhibit delamination defects in the range of 90°–180° for any fiber direction. In the process of fiber composite side milling, controlling the fiber cutting angle by controlling the radial cutting depth can reduce the occurrence of delamination defects effectively. Further fiber bending fracture model shows that the fiber is prone to bending fracture perpendicular to the workpiece in the FCA of 0°–90°. The bending fracture easily occurs in the plane of the workpiece in the range of 90°–180°. Hintze and Hartmann [55] considered only one type of surface layer

delamination, that is, fiber protrusion and fiber delamination always occurred simultaneously. The active force leads to the initial damage of the laminate, which can cause fibers to deflect instead of being cut off. Any fiber protrusion at machined edges is associated with delamination. Protruding fiber bundles lead to much deeper top layer delamination than protrusions of separate fibers. In addition to the anisotropy and non-uniformity of fiber composites, Azmi et al. [56] studied the tool wear mechanism and wear form in GFRP end milling and considered that the sharpness of the tool can affect the generation of delamination defects significantly. Hintze et al. [54] obtained a similar conclusion on the slot milling of CFRP. The wear tool with larger edge radius can significantly increase the defects, such as burr and delamination, on the machined surface.

2.3 Burr

When delamination occurs, the fiber is separated from the matrix. Some fibers with surface delamination were not completely cut off by the milling tool but by bending deformation. After the milling cutter leaves, the elastic deformation of the fiber recovers and forms burr defects. Figure 3 [31,57–59] shows the burr formation mechanism of fiber-reinforced composites in edge and slot milling. In the milling process, the surface fiber will be affected by the axial cutting force outward from the surface. When the axial force is greater than the interlayer bonding force in the milling process, the fiber will separate from the matrix and debond. Bending deformation occurs under the cutting force action after fiber peeling. Uncut carbon fibers will remain on the machined surface and form burrs because no material support is available outside the surface. The burr direction is generally consistent with the fiber direction [60]. Although high cutting speed and low feed rate are recommended for edge cutting of fiber composites, the situation is different in CFRP slot milling. In slot milling, the low thermal conductivity of the resin matrix tends to retain heat in the cutting area. This phenomenon leads to the softening, degradation, and combustion of the matrix that binds the fibers together. The softened matrix causes the flexible fibers to escape from the cutting edge and diffuse to a larger area, especially in the 90° and 135° directions [61]. Ghidossi et al. [62,63] also proved that tool wear was the main cause of burr in edge milling. Wang et al. [57] used cohesive elements to simulate interlaminar fracture and inserted bonding elements along the fiber direction into the top layer of CFRP to simulate interlaminar cracks. As shown in Fig. 3, burr and tear damage increase with FCA. When FCA is 0°, no burr exists, because the fracture of CFRP occurs in the cutting area, and the damage is eliminated. For 45°, 90°, and 135°, the crack caused by the failed cohesive element propagates to the unprocessed area along the fiber direction, so the fiber deformed easily and cannot be completely cut off. Uncut fibers remain above the machined surface to form burrs. The strong support effect of 45° fiber is just opposite to the weak constraint effect of 135°. Therefore, the burr length of 45° is shorter, and that of 135° is significantly longer. The UD-CFRP edge milling study by Wang et al. [58] showed that the thermal conductivity of fiber decreases with the increase in the angle between heat flow and fiber orientation, and the temperature is greatly affected by thermal conductivity. The cutting temperature of 45° is the lowest, and that of 135° is the highest. As shown in Fig. 3, when the fiber orientation is 45°, the optimal heat dissipation area is the largest, which can effectively reduce the temperature rise [58]. When the fiber orientation is 135°, the optimal heat dissipation area is the smallest, and losing a lot of heat is difficult. Resin degradation occurs on the cutting surface or surface when the cutting temperature exceeds the glass transition temperature. The fiber cannot receive enough support from the resin matrix, thereby resulting in the poor processing quality of the composite. The results of UD-CFRP slot milling by Kumar and Gururaja [31] showed that the milling temperature of 45° and 135° fiber orientation reached 160 °C. This result may be due to the decrease in thermal conductivity of 45° and 135° fiber-oriented UD-CFRP, which will increase the heat accumulation in the processing area. Due to the low thermal conductivity, the 135° fiber-oriented laminate has the largest heat storage area (yellow mark) and low heat dissipation area (green mark) (Fig. 3) [31]. He et al. [59] believed that burr and delamination are consistent, and its mechanism closely depends on the FCA. Due to the force on the fiber during chip formation, 90° is considered the critical angle for fiber cutting. As shown in Fig. 3, fiber bending will lead to serious burr and delamination in the top layer when FCA is at 90°–180°. Below 90°, fiber extrusion results in minimal or no burrs. However, in burr-free areas, machined surfaces usually have a poor surface finish. The damage also increases with speed when the feed rate per tooth is constant. Hou et al. [64] proposed that chatter was an important factor that affected milling surface quality, and the milling stability of CFRP was influenced by fiber direction. The milling stability is the best when FCA is 0° and the worst when FCA is 45°. When the fiber direction is 90° or 135°, the stability is between 0° and 45°. Compared with stable milling, burr, bulge, pit, and other defects are more likely to occur under chatter milling. The surface roughness of stable milling is reduced by 25%–53% compared with chatter milling.

2.4 Tear

When the residual burr is too long, the suspended fiber is stirred in by the milling tool and pulled with the tool feed. The root of the fiber will break, resulting in tearing

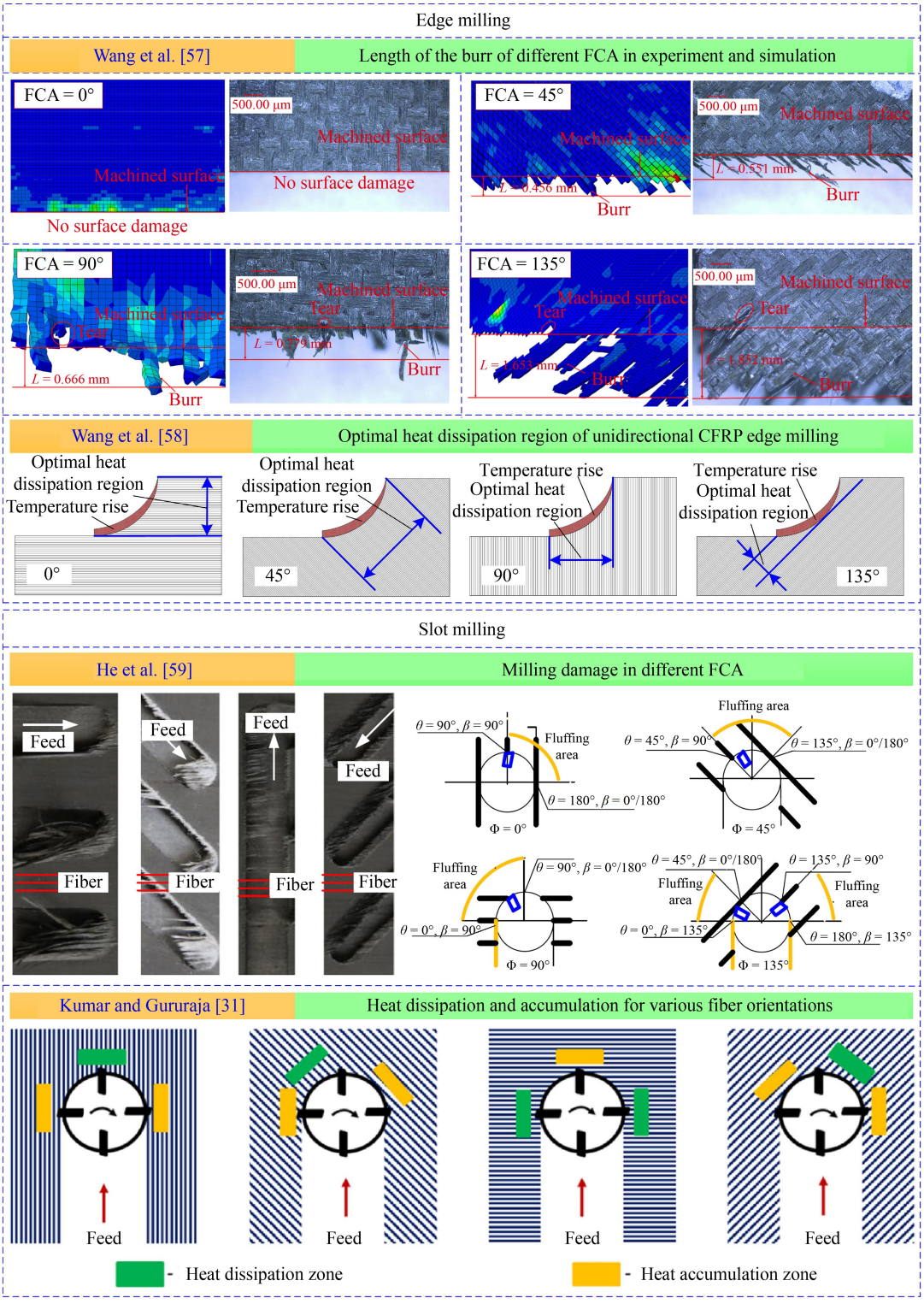

Fig. 3 Burr formation mechanism of fiber-reinforced composites in edge milling and slot milling. Reproduced with permission from Refs. [31,57–59] from Elsevier and Springer Nature.

defects when the tensile force is greater than the tensile strength of the fiber. Therefore, burr and tear are the further expansion of delamination defects and the macro embodiment of surface delamination. When the FCA is 90°–180°, the surface fiber is bent and broken by the milling tool, and the fracture crack penetrates into the surface material of the workpiece to form tear defects. If the residual burr is very long, then it is easily wounded by the tool teeth and breaks the fiber. The fracture position is generally deeper than the workpiece surface, and the tear

defect is formed on the workpiece surface. The cutting depth is affected by the tear angle and the sharpness of the cutting edge. The fiber layer is separated from the matrix material before tensile fracture because the axial tensile strength of the fiber is greater than the interlayer bond strength. The tearing direction is generally along the fiber. The tearing of the milled surface is generally accompanied by burr defects and has a similar evolution trend. During slot milling, serious resin coatings are found on the machined surface when the FCA is 0°–90°. Serrated fracture and tear defects appear on the machined surface when the FCA is 90°–180° [60]. The debonding and instability of CFRP surface material fiber is the cause of machining defects. According to the study of Wang et al. [57], CFRP milling with FCA of 90° and 135° has obvious tear damage. The stress extends to the machined surface along the fiber direction, resulting in the unpredictability of the location of stress concentration. The CFRP breaks below the processing area, resulting in tearing defects. More cracks propagate to the machined surface because the material is lifted under the bending stress at FCA of 135° and forms significant deformation. Therefore, the fibers easily break below the processing area, resulting in serious tearing. Therefore, 90° and 135° CFRP milling has poor surface quality, accompanied by burr and tear damage. The FCA has a significant effect on the milling force, stress, and material failure during the high-speed milling of carbon fiber cloth. The cutting force and stress follow the law of 90° > 135° > 45° > 0°. The anisotropy of fiber mechanical properties leads to different material removal forms, which is the main reason for the difference in cutting force. Under the cutting tool load, the fibers mainly exhibit shear failure and brittle removal. In addition, machining parameters play an important role in milling force, and single tooth feed rate is the most significant factor that affects milling force. At the same time, the progressive damage model predicts that the shear failure of materials is mainly concentrated in the shear region and extends along the feed direction [65].

3 Grinding mechanism

3.1 Material removal mechanism

The removal mechanism of fiber composites is complex because of the unique structural characteristics of heterogeneity, anisotropy, and multi-phase cross-scale composition. In addition, the inherent brittleness of ceramics and interface complicates the study of the fundamental mechanism of abrasive removal process [66]. Even more, the randomness of grains in grinding leads to more complex contact state and cutting behavior between grains and workpiece. Figure 4 [25,67–69] shows the material removal mechanism of fiber-reinforced composite grinding. Hu and Zhang [67] found that the fragments produced by multi-directional CFRP grinding showed a mixture of fine powder and broken fibers of different lengths (Fig. 4). This is different from unidirectional fiber-reinforced composite grinding. In UD-CFRP, the chip geometry mainly depends on the fiber orientation. The chips with 0° fiber orientation are mainly pulled out of broken fibers, and the chips with 90° fiber orientation are mainly fine powder. Qu et al. [70] showed that with the increase in grinding depth, a large number of damages was formed before the abrasive particles contact the fiber. Poor support conditions increased the debonding depth. The fracture surface of single fiber and fiber bundle becomes increasingly uneven and irregular. The grinding force and chip size increase gradually, and the grinding surface quality decreases gradually. According to Liu et al. [68] in the grinding of 2-dimensional (2D) C/SiC composites, the failure forms are mainly the combination of fiber fracture, matrix fracture, and interface debonding (Fig. 4). The grinding debris is composed of carbon fiber debris, carbon powder, and SiC matrix debris. The main removal mechanism of 2D C/SiC composites is brittle fracture. Zhang et al. [71] reached the same conclusion on the failure form of material removal in unidirectional C/SiC composite grinding. Yang et al. [72] found that most fibers and matrix were broken into fine debris during the grinding of unidirectional C/SiC. The average crack depth and the average length of debris increase gradually with the cutting depth. However, two completely different kinds of debris are formed in the grinding of 2.5D C/SiC. The appearance and size of warp wear debris are very similar to those of unidirectional C/SiC. The crack is more likely to propagate along the fiber direction in the weft, indicating the formation of long and large fiber debris. Further, Liu et al. [73] analyzed the grinding mechanism of 2D C_f/C-SiC composites by single grain scratch test. The fiber bundle is damaged by the combined action of peeling and tearing, which depends on the FCA. The material removal mechanism is mainly brittle removal, that is, the combination of fiber layered brittle fracture and SiC matrix cracking. The influence of carbon fiber on machining results is greater than that of matrix material. In each cutting mode, matrix cracking, matrix/carbon fiber bonding, carbon fiber fracture, and other phenomena occur, thereby resulting in the brittle spalling of the material. Different cutting methods have various effects on chip width, and the order of chip width is $\perp > \parallel > \odot$. Fibers scratched in the $\perp$ and $\parallel$ directions are often removed as blocks by peeling or pushing away [74]. Li et al. [75] reached a similar conclusion in the single grain scratch test and considered that the cutting force and direction would affect the failure mode and subsurface influence zone of the material. Garcia Luna et al. [25] studied the effects of grain shape, size, spacing, and fiber direction on the material removal mechanism of

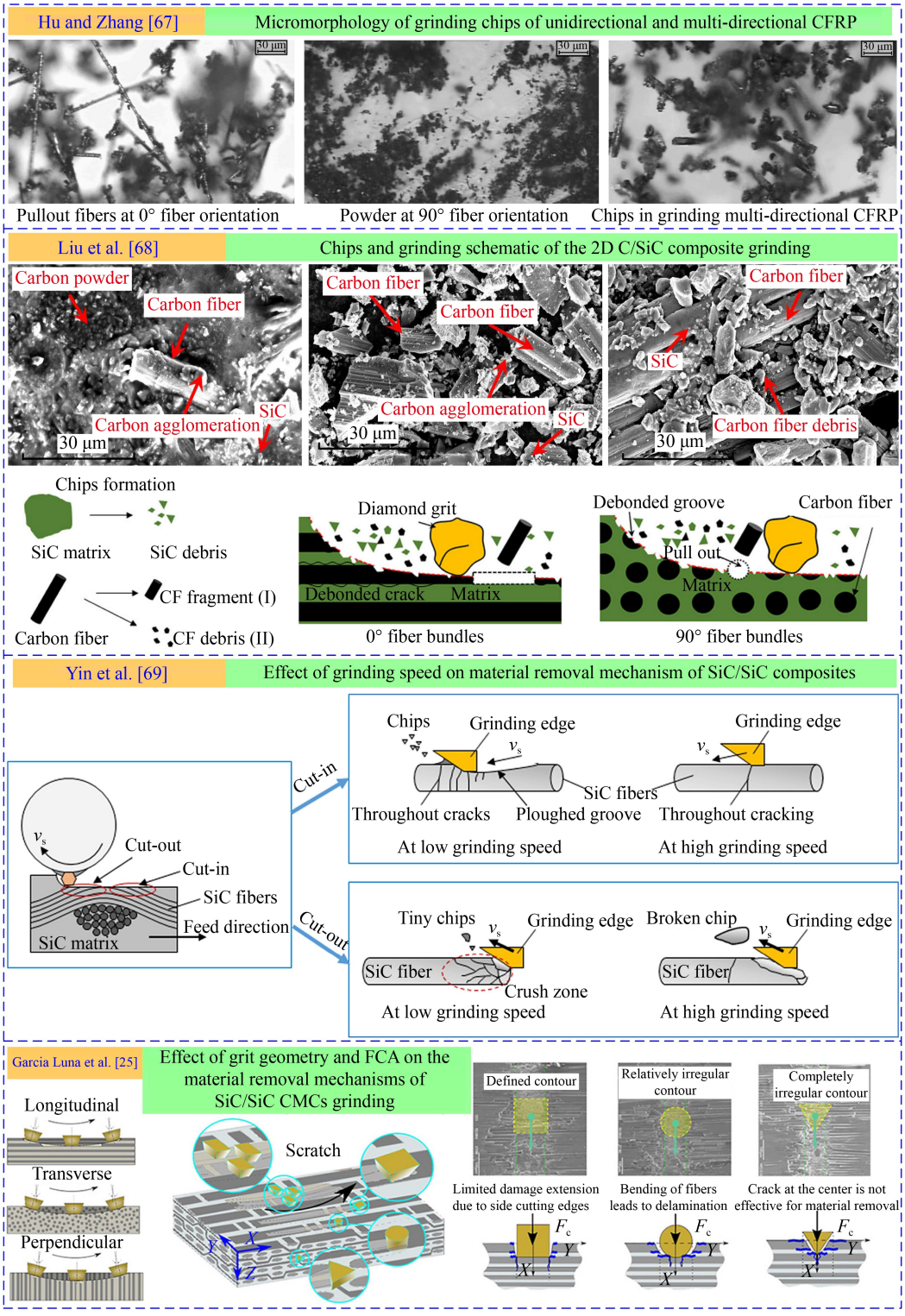

Fig. 4 Material removal mechanism of fiber-reinforced composite grinding. Reproduced with permission from Refs. [25,67–69] from Elsevier and Springer Nature.

SiC/SiC composite grinding through a single grain scratch test (Fig. 4). The results show that the grain shape has a greater influence on the force than the fiber orientation because of the removal of brittle materials. Circular grain produces greater thrust than square and triangular grains because it has no stress concentration points. However, square grain shows excellent ability in reducing transverse damage of transverse fibers. The grain shape determines the location of cracks, and the fiber orientation determines the subsequent crack

propagation, and preferentially along the interface direction. Yin et al. [69] studied the effect of grinding speed on the material removal mechanism of SiC/SiC using single grain (Fig. 4). The results show that increasing the grinding speed can embrittle the material and strengthen the fracture of fiber. When grinding along the warp direction of the fiber, the fiber shows brittle fracture, and the matrix is torn during high-speed grinding. No fiber ploughing or substrate coating is observed in low-speed grinding. When grinding transversely along the fiber warp direction, increasing the grinding speed can completely remove the fiber, and a little cut fiber residue is found on the bottom surface of the groove, which improves the surface finish. Increasing the grinding speed can also improve the removal rate of SiC/SiC composites. Wei et al. [76] conducted the frequency component analysis and damage pattern recognition of acoustic emission signals from 3D orthogonal SiO_2/SiO_2 composite grinding. The results show that the main sources of acoustic emission are fiber fracture, matrix crack, and debonding between fiber and matrix. The grinding study of 2.5D woven SiO_2/SiO_2 composite by Wang et al. [77] showed that crack propagation and material breakage can be found in the grinding area. The main removal mechanism is brittle fracture, which is similar to brittle homogeneous materials [78,79]. Inoue and Kawaguchi [80] clarified the grinding mechanism of GFRP. Two internal failure modes are observed near the surface of the fiber bundle. One is the mode, in which deeper fiber debonding unfolds in the whole fiber bundle. The other is that the failure in the fiber bundle is relatively shallow and random in terms of depth and expansion, often in the form of needle cracks. There are two kinds of fiber bundle cutting profiles. One is the pit formed by the protruding fiber bundle under the action of digging up during grinding, and the other is the expansive bulge composed of uncut glass fibers. Chockalingam et al. [81] showed that the protruding fibers are still obvious in GFRP dry grinding, although the surface is covered with broken matrix. The surface ground with synthetic coolant is clean, hard, and smooth. Chockalingam and Kuang [82] compared the GFRP grinding performance of alumina grinding wheel and cubic boron nitride (CBN) grinding wheel. The results show that the grinding force ratio and machining efficiency of CBN grinding wheel is generally higher than that of alumina, and the grinding surface roughness is lower in most cases.

3.2 Thermal and mechanical behavior

Grinding force is an important index to investigate the influence of machining parameters on grinding performance [83]. It results from the elastic and plastic deformation of the workpiece and the interaction among grains, materials, and debris [84,85]. It involves almost all factors of grinding and is the basis of researching grinding technology, designing appropriate cutting tools, and selecting appropriate machine tools. It is also an important index to evaluate the processing characteristics of materials. Figure 5 [74,75,83] shows different grinding experimental equipment of single grain. Figure 6 [71,74,77,86] shows the mechanical behavior of fiber-reinforced composite grinding. The grinding force of fiber composites is also highly dependent on the fiber orientation [86]. Zhang et al. [71,87] investigated the grinding forces in three typical grinding directions of unidirectional C/SiC composites. The grinding force follows the order: normal > longitudinal > transverse. Li et al. [75] designed a novel scratch test equipment (Fig. 5). The results show that the tangential force (F_t) is generally greater than the normal force (F_n) at the same cutting depth. In the longitudinal scratch direction, the carbon fiber is mainly pulled out and bonded with the fractured SiC matrix. In the transverse scratching, the carbon fiber is mainly cut off and slightly pulled away laterally with the fractured SiC matrix. The longitudinal cutting force is greater than the transverse cutting force because of the high axial Young's modulus, and the carbon fiber transmits its stiffness and resistance to the fiber direction. The grinding force of multi-directional CFRP (MD-CFRP) increases approximately linearly with the grinding depth and is generally greater than those of UD-CFRP composites. The reason may be that the layers with different fiber orientations have stronger mutual support [67]. The grinding force increases with the feed speed and cutting depth and decreases with the increase in grinding wheel speed. Under the same experimental conditions, the force ratio (F_n/F_t) and specific grinding energy of 2D C/SiC composites are lower than those of traditional ceramics [68], such as Al_2O_3, SiN_4, ZrO_2, and SiC ceramics [88,89]. This result may be due to the introduction of brittle carbon fiber material, which causes the 2D weave C/SiC composite to have higher brittleness and easily damaged, so that its force ratio is lower than that of traditional ceramic materials. According to the weave and laminated structure of fiber bundles, Liu et al. [74] selected three typical surfaces (e.g., SA, SB, and SC) for scratch test (Fig. 5) under different scratch speed and depth combinations. Under different scratch modes, the order of the maximum scratch force is normal > transverse > longitudinal, and the order of the average scratch force on the three surfaces is SB > SA > SC (Fig. 6). Under the same grinding parameters, the grinding force of 2.5D C/SiC is always greater than that of UD-C/SiC [72]. Considering that the weak coupling force between unidirectional fibers promotes the crack propagation further. In 2.5D C/SiC, the orientation of warp and weft yarns changes under the action of needle structure, which shows that the coupling between fibers is effective in obtaining higher strength. Wang et al. [77] found that the grinding of 2.5D woven SiO_2/SiO_2 composite can

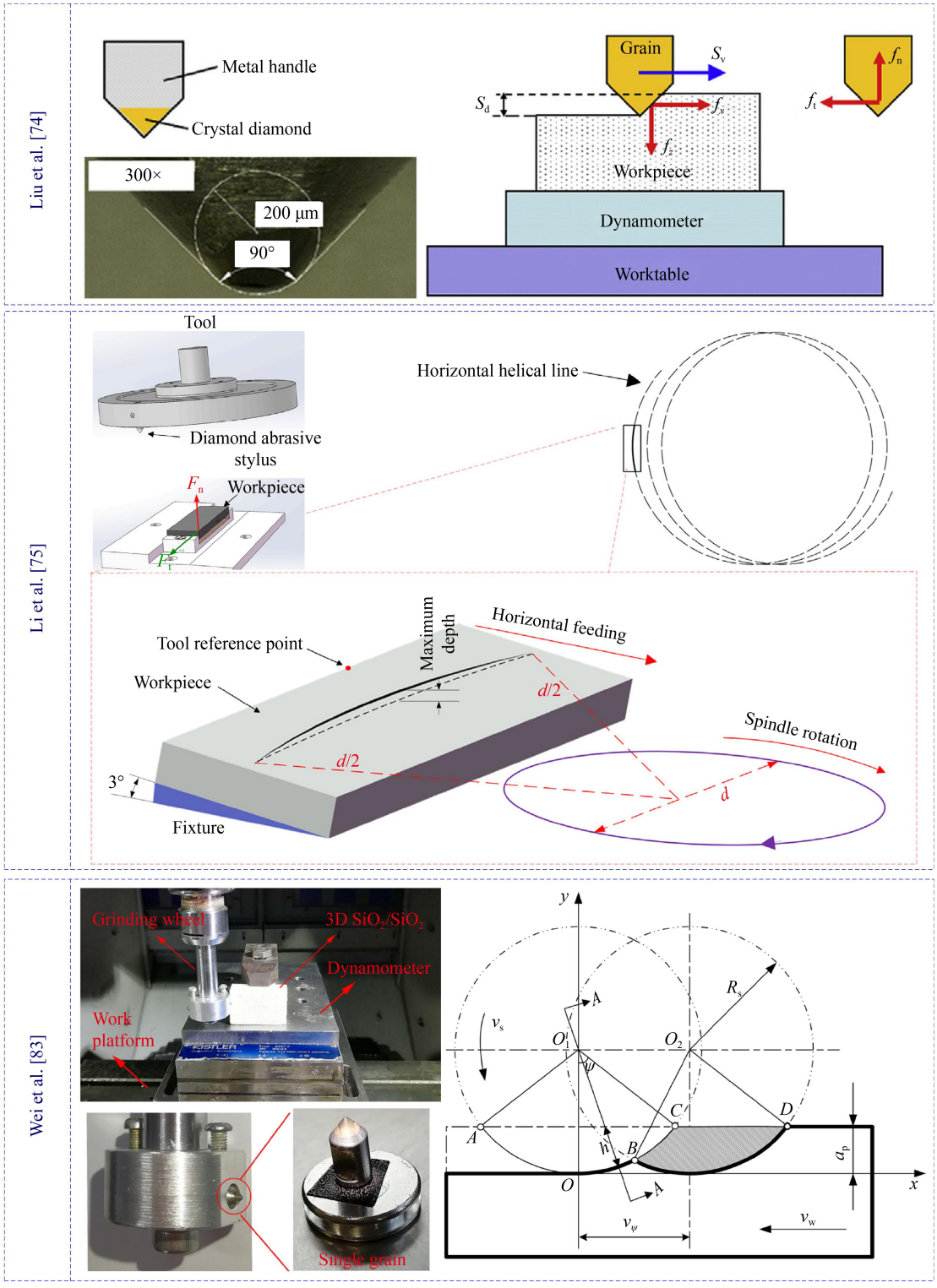

Fig. 5 Various experimental devices of single grain grinding. Reproduced with permission from Refs. [74,75,83] from Elsevier and Springer Nature.

travel along the fibers. Therefore, for 2.5D woven SiO_2/SiO_2 composite, the influence range of grinding process is wider than that of other materials. As shown in Fig. 6, only shear stress is generated on the fiber without tensile stress in the grinding direction of B2 and C2. Thus, the matrix is less damaged [77]. Cao et al. [86] found that the material removal of 2.5D woven SiO_2/SiO_2 composite was mainly caused by shear fracture and open crack when FCA = 0°. The force that separates the fiber/matrix interface is small, because the bonding

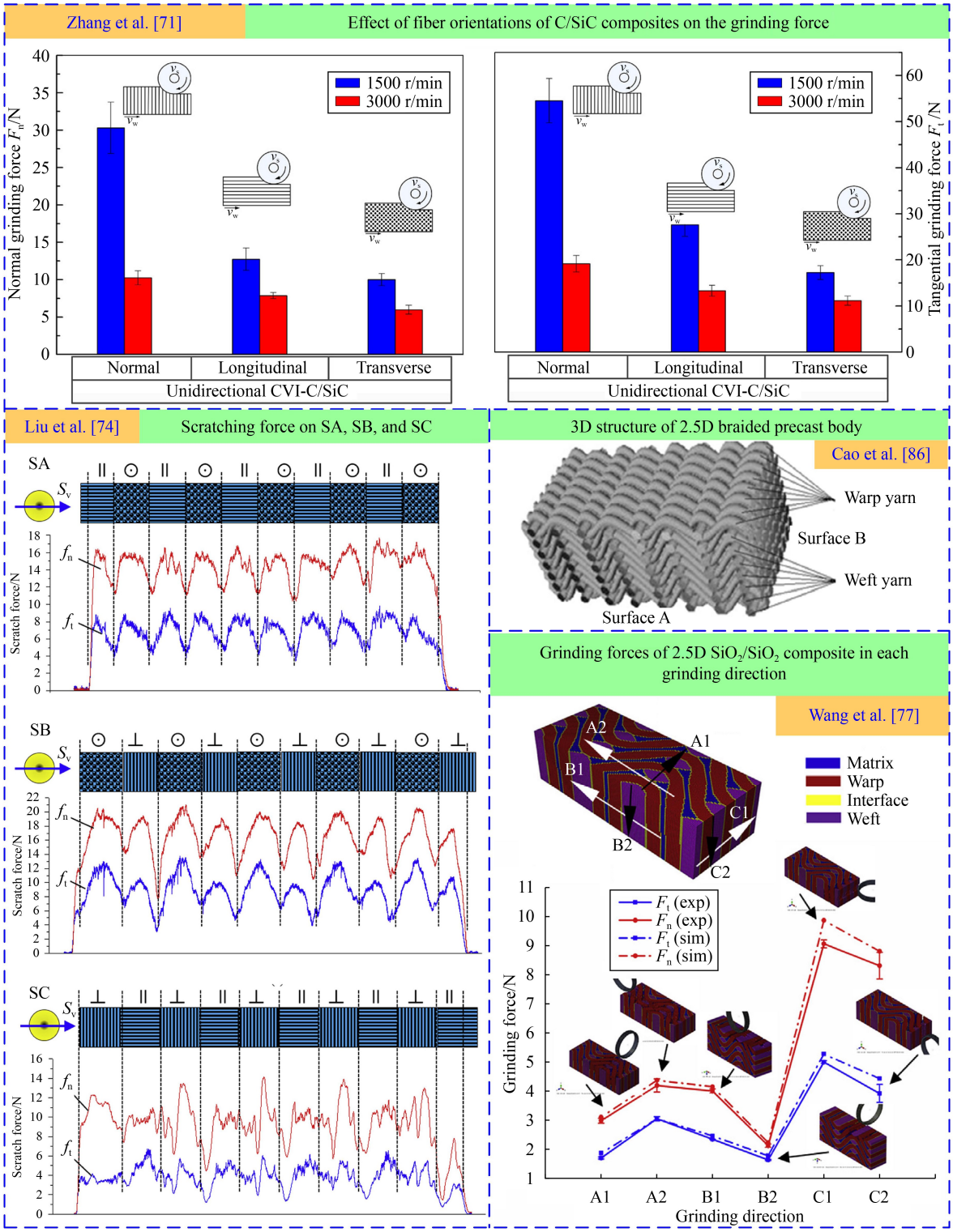

Fig. 6 Mechanical behavior of fiber reinforced composites grinding. Reproduced with permission from Refs. [71,74,77,86] from Elsevier.

strength between fiber and matrix is much lower than fiber strength. The material removal involves the shear fracture of fibers with the increase in FCA, and the grinding force increases due to the high shear strength of fiber. The vertical grinding force is the largest when FCA = 90°, because the fiber has the highest longitudinal strength and the resistance to the vertical compression of the grinding wheel increases. According to the weaving method (Fig. 6) [86], the proportion of weft fiber is less than that of warp. Therefore, the normal grinding force of

surface B is larger than A. The supporting conditions and debonding depth are the key factors that affect the grinding force. According to the interaction of forces, Qu et al. [70] decomposed the grinding force model of C/SiC composites into the mechanical model of the fracture area of the SiC matrix and the formation area of the fiber grinding chips. Based on energy balance theory, Wei et al. [83] modified the specific grinding energy model, combined with the single abrasive experiment of 3D orthogonal SiO_2/SiO_2 composite (Fig. 5) and proposed a new semi-analytical force model of single grain grinding force. Liu et al. [90] found that the grinding force remained basically unchanged with the increase in grinding wheel particle size. The reason is that with the increase of particle size, the particle size of abrasive particles decreases while the number of active abrasive particles increases, resulting in slight changes in grinding force. Kodama et al. [91] believed that carbon fiber composites produce two-stage heat affected layers during grinding. First, the heat affected layer of the glass transition of the resin matrix, and the heat affected layer of the thermal replacement of the matrix resin are generated. The thermal deformation of matrix resin deteriorates the characteristics of grinding surface. From the point of view of machining quality and machining damage degree, small equivalent chip thickness trimming is the most suitable [92]. Under fine machining conditions (e.g., minimum equivalent chip thickness, minimum cutting depth), no edge delamination and internal damage occurs. Fan et al. [93] established the simulation model of CFRP grinding heat distribution ratio and found that the grinding heat was preferentially conducted along the fiber because the thermal conductivity of fiber is obviously greater than that of resin. The resin surface temperature is higher because the thermal conductivity of the resin is low. Sheikh-Ahmad et al. [94] proposed that inverse heat conduction method was an effective and efficient technique for determining the energy balance in machining CFRP. Qian et al. [95] found that the heat generation mechanism at 90° was more complex compared with 0°, resulting in the highest cutting temperature when the FCA was 90°. The thermal damage depth is the minimum at 0° and the maximum at 90°.

3.3 Surface integrity and damage

The damaged carbon fibers in the grinding of CFRPs include fiber pullout, voids, partially cut fibers, breakage and fracture of carbon fibers, and flowed matrix [96,97]. The surface roughness of MD-CFRP changes with the fiber's local orientation, and there are serious fiber pullout and other damage in 135° layer [67]. Hanasaki et al. [98] investigated the grinding of UD-CFRP and MD-CFRP and found an interesting phenomenon. As shown in Fig. 7 [77,97,98], the workpiece surface roughness in the 90° direction is the smallest, and the surface roughness in the 135° direction is the largest during UD-CFRP grinding. However, the surface roughness of MD-CFRP composed of 45°/135° is less than that of UD-CFRP. The explanation for this phenomenon is detailed as follows. The unidirectional carbon fiber of 135° is bending and fracture, and the fracture point is unstable. However, the combination of 45° and 135° carbon fibers can stabilize the fracture point. Soo et al. [99] found that tool wear, cutting force, and surface roughness were high using CBN abrasive for CFRP laminate edge grinding compared with diamond abrasive. The resulting damage includes slight edge fracture/chip and pores caused by fiber/matrix loss. The damage caused by both abrasives includes slight edge fracture/chip and pores caused by fiber/matrix loss. However, there is no obvious large-scale delamination in the two kinds of superbrasive coatings. From the surface micromorphology, matrix cracking, fiber pullout, and fiber outcrop are the main damage forms in the grinding of unidirectional C/SiC composites. In the grinding process, the debonding depth between matrix and carbon fiber depends on the sharpness and lubrication state of grains [100]. Using mechanical damage phenomenology, Cao et al. [101] analyzed the formation mechanism of grinding surface ripple of CMCs composites. Fiber orientation plays a decisive role in waviness, which is different from the traditional theory of ripple formation caused by the vibration of machine tool system. Zhang et al. [71] found that the surface roughness of arithmetical mean deviation of the profile R_a and maximum height of the profile R_z of unidirectional C/SiC composites in grinding directions follow the order of longitudinal > normal > transverse. Fiber pullout and fiber outcrop are the basic damage modes of unidirectional C/SiC. Interface peeling, matrix cracking, fiber pullout and fiber outcrop are the main defect forms of 2.5D C/SiC. Compared with unidirectional C/SiC, the subsurface damage of 2.5D C/SiC is shallower and wider [72]. Wang et al. [77] considered that the surface damage of 2.5D SiO_2/SiO_2 composites mainly resulted from matrix crushing and fiber debonding. Matrix breakage is caused by two reasons: 1) The matrix is weak and damaged by grinding force; and 2) the matrix is squeezed by fibers (Fig. 7). The latter plays a greater role because it cannot only destroy the matrix in the grinding area but also destroy the matrix in the area far away from the grinding area. In the aspect of fiber debonding, there have been studies on the influence of fiber orientation on the cutting process and the damage of fiber debonding on the machined surface [71,86,102]. However, these studies ignore the interaction among fiber bundles. Wang et al. [77] considered that the difference of warp and weft fiber bundle deformation capacity was the key factor that affected the overall deformation. The weft bundle is only inserted into the gap to form a weak connection. When

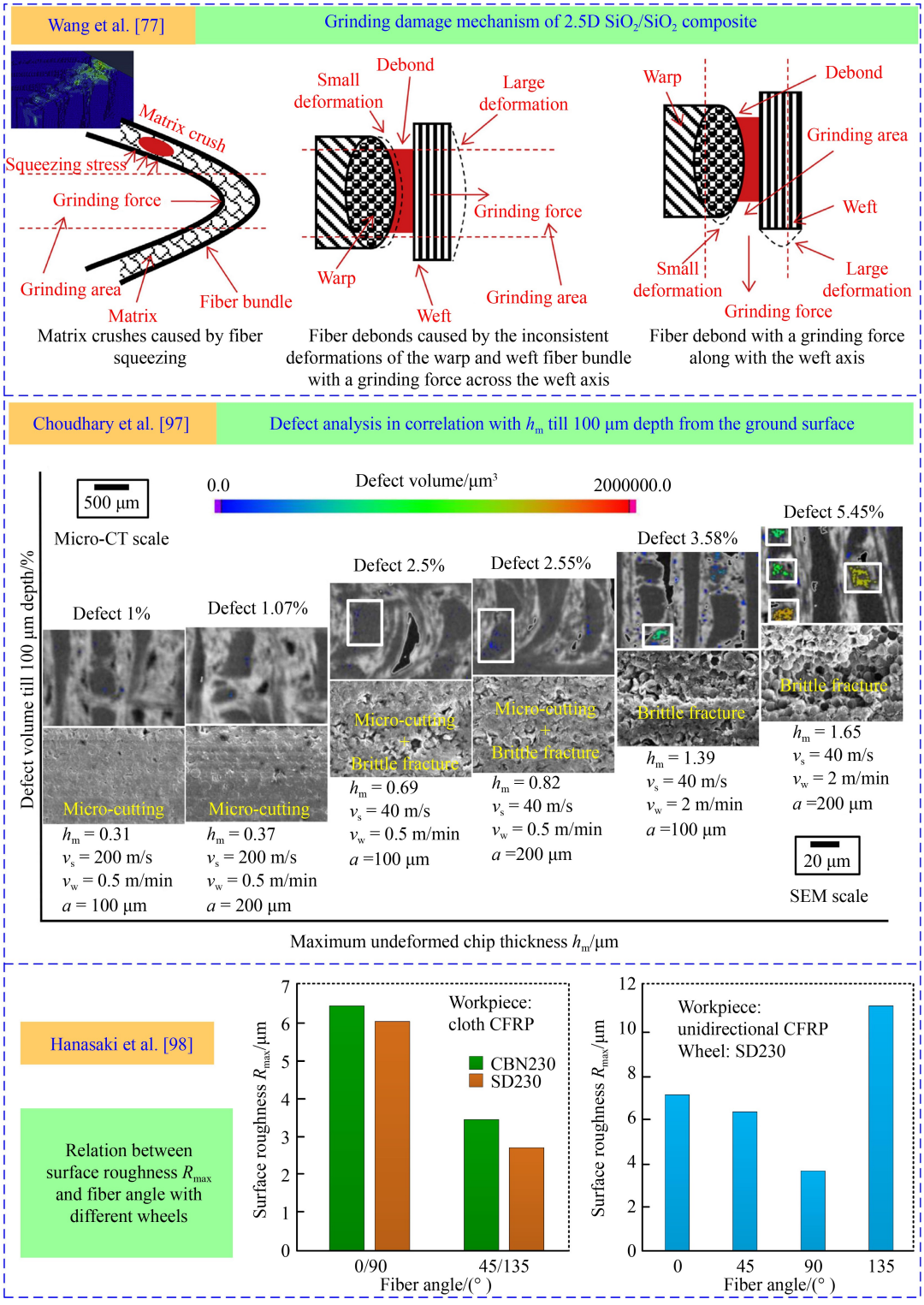

Fig. 7 Grinding damage mechanism and surface roughness trend. Part of the figure was drawn based on Ref. [98]. Reproduced with permission from Refs. [77,97] from Elsevier.

the grinding force is in the direction shown in Fig. 7, the weft fiber produces greater deformation than the warp fiber bundle. Then, the bonding connection between warp and weft is destroyed, thereby forming mechanical damage on the fiber bonding. Fiber debonding usually appears as a slight tear in the grinding area, and its damage to the surface quality is less than that of matrix breakage. Therefore, grinding along the weft axis is a better choice to reduce fiber debonding. Transversely oriented fibers are subjected to high normal force during

grinding, thereby resulting in crack propagation along the fiber direction and delamination. Choudhary et al. [97] proposed that the grinding scallop and the chip thickness of the cutting surface determine the characteristics and degree of fiber damage (Fig. 7). The crack deflection mechanism plays an important role in the orientation of fibers and limits the delamination of fiber matrix. High-speed grinding reduces the maximum undeformed chip thickness and grinding scallop and promotes the shear micro cutting of fiber and matrix rather than brittle fracture. High-speed grinding process is effective in machining defect-free C/SiC CMCs. Fiber orientation plays a key role in the grinding of surface micromorphology of SiO_2/SiO_2 composite [103]. Grinding speed has the greatest influence on height and surface support performance, followed by grain size and depth of cutting. Grain size is the key factor that affects the change in surface micromorphology. Cao et al. [86] also believed that the grinding speed and cutting depth had a great influence on the surface morphology. The surface topography height decreases with the increase in grinding wheel speed, and the deflection of topography distribution decreases with the increase in grinding depth.

4 Advanced cutting tools and technologies

4.1 Ultrasonic vibration assisted machining

Ultrasonic vibration-assisted machining (UVAM) is one of the newly developed machining technologies [104–106]. It is a machining method that combines ultrasonic vibration with traditional machining [107,108]. It adds high-frequency ultrasonic vibration to the tool or the workpiece, uses the energy of ultrasonic vibration to change the removal mechanism [26], improve the machining process, and obtain better machining performance [109–111]. Figure 8 shows the damage suppression mechanism of ultrasonic vibration grinding [112–115]. UVAM adds a microscale amplitude displacement with ultrasonic frequency to the tool tip motion [116,117] and changes the path of the tool tip so that the instantaneous cutting depth is much smaller than the fiber diameter, which can improve the surface integrity [118,119]. UVAM with horizontal ultrasonic vibration generated fewer defects because of abrasive-grain trajectory overlapping. The smaller simultaneous depth of cut and smaller simultaneous cutting volume in UVAM contributed to the less severe fiber fracture, cracks, and damages on matrix in processing fiber composites [120,121]. UVAM has a significant effect on reducing cutting force, and the cutting force needs to be predicted and modeled for its controllability and minimization. The modeling of cutting force is also the key to effectively control the machining damage of fiber composites. However, due to the heterogeneity, anisotropy, and low heat dissipation characteristics of these composites, ensuring high accuracy and low estimation error of the force model is difficult. Amin et al. [122] established the axial and feed cutting force models of CFRP composites and characterized and calculated the exposed height of diamond grains in the modeling process. Furthermore, the force models of CFRP ultrasonic-assisted surface milling of two milling tools (cylindrical abrasive core tool and conical shaped core tool) are established [123]. The expression of tool contact area is improved, and overlapping cutting quantification is introduced for the first time. The estimation error between the experimental and simulated values of cutting force is less than 10%. In recent years, ductile material removal mode and brittle mode can be applied in CFRP ultrasonic vibration-assisted grinding (UVAG). Wang et al. [124] established the force model of ultrasonic vibration-assisted edge surface grinding of CFRP composites based on ductile and brittle mode and used the critical indentation depth to distinguish plastic and brittle zones. The plastic zone increases, and the brittle zone decreases with the increase in tool speed or the decrease in feed rate. The brittle region increases with the cutting depth. Rotary ultrasonic machining using vertical ultrasonic vibration is an effective method to reduce the cutting force. However, the quality of the machined surface decreases due to the knocking effect of vertical vibration on the machined surface. Based on the removal mechanism of brittle fracture materials, Wang et al. [13] established a CFRP grinding force model under horizontal ultrasonic vibration. The results show that the grinding force decreases with the increase in ultrasonic amplitude. Ning et al. [125] established a feed force model for CFRP surface grinding based on the material removal hypothesis of brittle fracture, by introducing the fracture volume factor of awesome material. The difference in the fracture behavior of carbon fiber leads to the difference in the material removal energy consumption. The difference of material removal mechanism directly leads to the difference of machined surface morphology. The material removal mechanism can be effectively characterized by machined surface roughness. Chen et al. [112] considered that the transformation of material removal mechanism depends on the maximum undeformed chip thickness (h_{max}). Micro cracks are generated and propagated in the carbon fiber because of the extrusion of abrasive particles when h_{max} is small enough. SiC matrix breaks and carbon fiber debonds from the matrix when h_{max} is large enough. The main fracture mechanisms are bending fracture, compression fracture, and shear fracture. As shown in Fig. 8, UVAG promotes the removal of carbon fiber in nano brittle fracture by reducing the maximum undeformed chip thickness to improve the machined surface quality [112]. The improvement effect increases with the amplitude. Ding et al. [113] considered that UVAG reduced the layered

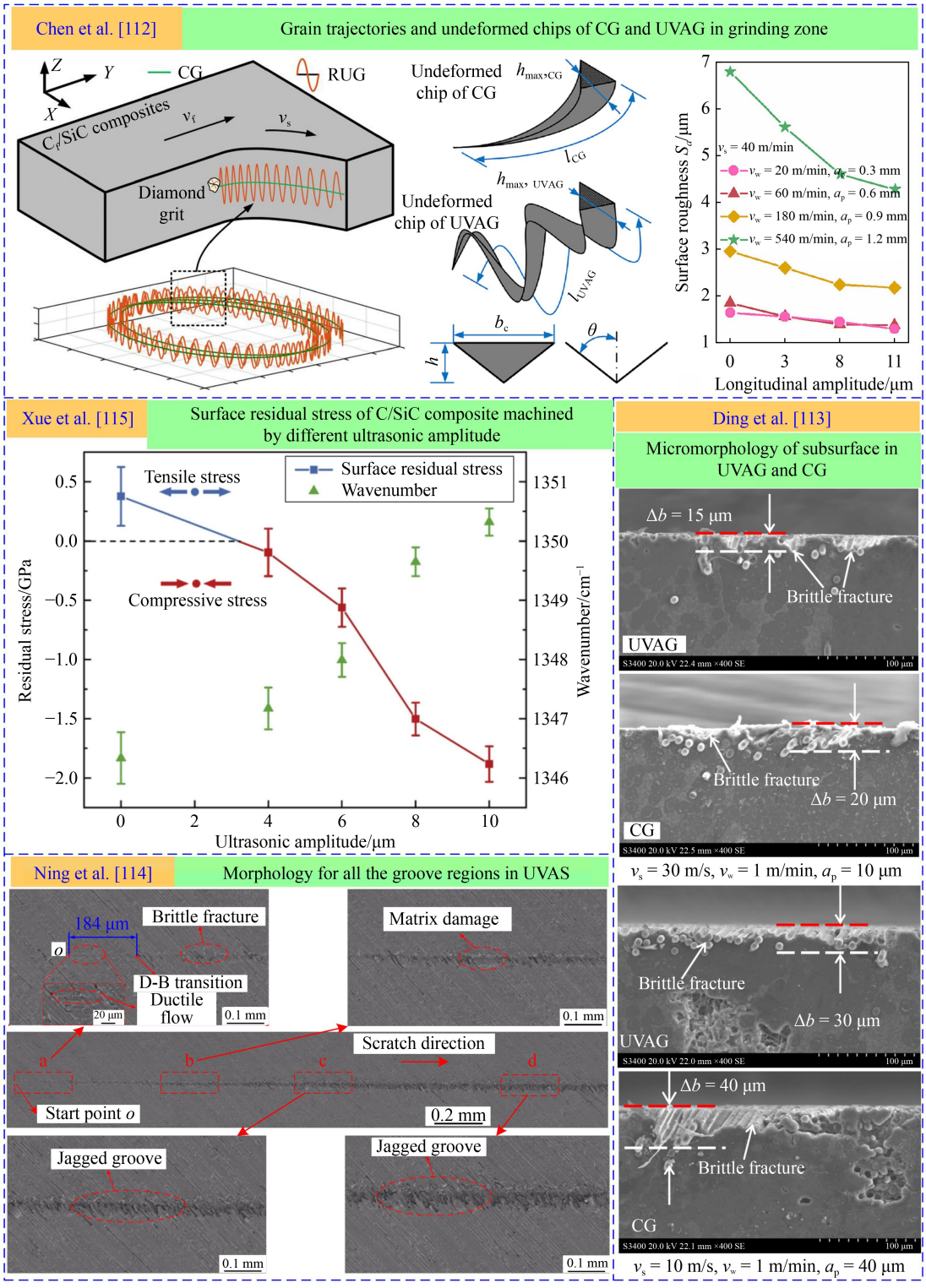

Fig. 8 Damage suppression mechanism of ultrasonic vibration assisted machining. UVAS: ultrasonic vibration-assisted scratching. Reproduced with permission from Refs. [112–115] from Elsevier and Springer Nature.

brittle fracture and pit group caused by fiber fracture and pull-out to varying degrees compared with conventional grinding (CG) because UVAG could reduce the grinding force that determined fiber fracture. Therefore, due to less fiber breakage and reduction of fracture size (Fig. 8 [112–115]), the surface roughness of arithmetical mean deviation of regional morphology S_a obtained by UVAG is lower than CG, with a maximum decrease of 12% [113]. Wang et al. [96] reported the influence of machining variables (e.g., ultrasonic power, grinding

speed, feed rate and depth of cutting) on output variables (e.g., cutting force, torque, and surface roughness). The results show that increasing the ultrasonic power and grinding speed and decreasing the feed rate can reduce the force and the depth of damage. The surface roughness can be lessened by reducing ultrasonic power, feed rate, and cutting depth and increasing grinding speed. The up-grinding force is evidently greater than that of down grinding, and down grinding produces low surface roughness. Li et al. [126] discussed the reasons for the differences in cutting force and surface integrity. The surface morphology shows that brittle fracture is the main material removal mode of CFRP composite grinding. The chip size of the resin, the fracture size of carbon fiber, and the material removal size are small using down grinding. Therefore, ultrasonic vibration-assisted down-grinding CFRP is the optimal scheme to obtain high surface quality and the required dimensional accuracy. Wang et al. [127] found that ultrasonic vibration-assisted milling along 90° orientation can obtain less cutting force and torque. The main reason is that when the machining orientation is 0°, the tool continuously cuts carbon fiber layers, accelerate the tool passivation, and increase the friction between the tool and the workpiece. The tool can alternately cut carbon fiber and epoxy resin in the FCA of 90°. Smaller surface roughness can be obtained in 0° because the fiber is not successfully cut in 90°, thereby resulting in fiber pulling out and burr. The heavier the fracture of the carbon fiber is, the more chips and cracks are produced. Ning et al. [114] found that CFRP was brittle removed, resulting in matrix damage and serious fiber pullout and macro cracks in the conventional scratch test. However, ultrasonic vibration-assisted scratching (UVAS) of CFRP has a large ductile removal area before continuous brittle fracture and crack. Debonding and pulling of fiber matrix are also significantly reduced, and only matrix buckling and fiber fracture occur in the groove (Fig. 8 [114]). Xue et al. [115] showed that the surface residual compressive stress of C/SiC composites is approximately 2 GPa because of the continuous impact of high-frequency and low-amplitude vibration (Fig. 8). Residual compressive stress restrains most of the interface cracks and hinders the propagation of fiber cracks to improve the toughening effect and machined surface quality of fiber. The surface quality of fiber composites is closely related to the fracture mechanism [128]. High-frequency and low-amplitude vibration changes the cutting angle of the fiber and increases the shear stress of the fiber through the axial to radial deflection friction of the fiber. It greatly promotes the transformation from shear fracture mode to dominant fracture mechanism. Ultrasonic vibration increases the proportion of FCA under shear fracture mode by 30%. Table 1 [13,90,96,104,112–115,120,122–144] shows the vibration parameters of ultrasonic vibration and their comparison with the results in traditional machining.

4.2 Cryogenic cooling

The temperature in the cutting area increases rapidly due to the machining process because of the low thermal conductivity of the composites. The processing damage intensifies, especially in the machining of resin matrix fiber composites when the cutting zone temperature reaches the glass transition temperature of the resin matrix [145]. Therefore, controlling the cutting zone temperature in an appropriate range is crucial in improving the machining quality [146–149]. Jia et al. [150] first proposed the concept of cutting CFRP at appropriate temperature (–10–25 °C). The quality of low-temperature processing is generally better than that of high-temperature milling. The micromorphology of fiber at high temperature shows bending fracture and serious sub surface damage. In contrast, the low-temperature hardening matrix provides better support for the fiber, and the composite is easily extruded and broken. However, the cutting force increases sharply, and the tool life decreases when the temperature is too low. Conversely, Zhang et al. [151] demonstrated that the tool life of polycrystalline diamond (PCD) and chemical vapor deposition (CVD) diamond tools in cryogenic milling SiC/SiC were two and four times higher than that of dry machining, respectively. The metal bond of cobalt (CO) in PCD tools increases its fracture toughness, thereby resulting in different service lives of the two tools. Kumar and Gururaja [31] demonstrated the change in fiber fracture mode and the integrity of machined surface during low-temperature (liquid nitrogen, LN_2) machining. Under the condition of cryogenic cooling, shear failure is dominant at 135°, tensile failure at 90°, and tensile failure and compression failure at 45° (Fig. 9 [31,158]). Surface damage, such as the attached fiber/matrix dust particle, fiber fracture, cavities, fiber/matrix de-cohesion in dry condition, and pull-out of fibers in cryogenic conditions, were the governing factors in 45° fiber orientation. Cryogenic cooling reduced fiber/matrix debonding. Nor Khairusshima et al. [152,153] applied –10 °C chilled air (air pressure of 0.55 MPa, flow velocity of 4.10 m/s) to cutting tools using vortex tube. Compared with room-temperature milling, chilled air can reduce heat generation and tool wear significantly to obtain lower surface roughness and delamination factor. Danish et al. [154] explored the milling performance of CFRP in continuously lubricated cooling media (e.g., dry, MQL, cryogenic liquid nitrogen, and CO_2). LN_2 and CO_2 are very successful in reducing grinding force, surface roughness, cutting temperature, and tool wear [155]. The contribution of lubricating cooling medium in reducing cutting force, tool wear, surface roughness, and cutting temperature is 49%, 46%, 38.89%, and 50.21%, respectively. Zou et al. [156] applied supercritical CO_2 to CFRP milling, which avoided thermal damage and improved surface quality effectively. The effects of cryogenic

Table 1 Ultrasonic vibration parameters and output parameters

Reference	Vibration mode	Amplitude/μm	Frequency/kHz	Composites	Output parameters (compared with CM)
Wang et al. [13]	1D horizontal	2; 4; 5	28	UD-CFRP	–
Liu et al. [90]	1D longitudinal	10	20	MD-CFRP	–
Wang et al. [96]	1D longitudinal	–	20	UD-CFRP	–
Xu et al. [104]	Longitudinal–torsional	6; 3	22.5	AFRP	Cutting force: ↓ 15%–48%
Chen et al. [112]	Longitudinal–torsional	Longitudinal amplitude (LA)/torsional amplitude (TA) = 14/5; LA = 3; 8; 11	19.3	2D C/SiC	Specific grinding energy: ≈ ↓ max 50%; S_a: ≈ ↓ max 38%
Ding et al. [113]	1D longitudinal	3.85	21.5	2D C/SiC	F_n: ↓ 9%–21%; F_t: ↓ 9.7%–19.4%; S_a: ↓ 6.6%–12%; Fracture size: ↓ 25%
Ning et al. [114]	Horizontal–vertical	3	20	MD-CFRP	–
Xue et al. [115]	1D longitudinal	4; 6; 8; 10	20	3D C/SiC	Standard deviation of height of each point in the area S_q: ↓ 37.9%; fatigue damage rate: ↓ 31%–80%
Wang et al. [120]	Horizontal; horizontal–vertical	Horizontal 4; vertical 6	28; 20	CFRP	Cutting force: ≈ ↓ 21%–36%; surface roughness: ≈ ↓ 50%–62%
Amin et al. [122,123,129]	1D longitudinal	10	16; 20.5	MD-CFRP	–
Wang et al. [124]	1D longitudinal	4; 6; 7; 8	20		–
Ning et al. [125]	1D longitudinal	4; 5; 6; 7; 8	20	MD-CFRP	–
Li et al. [126]	1D longitudinal	6	20	MD-CFRP	–
Wang et al. [127]	1D longitudinal	–	20	MD-CFRP	–
Xue et al. [128]	1D longitudinal	10	20	3D C/SiC	Distance between the highest and lowest points of the contour R_t: ↓ 37.5%; R_a: ↓ 32.4%; R_z: ↓ 32.8%
Yuan et al. [130]	1D longitudinal	10; 15	–	MD-CFRP	–
Liu et al. [131]	1D longitudinal	2; 4; 6; 8; 10	21.19	C/SiC	F_x: ↓ 43.7%; F_y: ↓ 9.16%; F_z: ↓ 68.09%; R_a: ≈ ↓ 12%–16.7%
Chen et al. [132]	Longitudinal–torsional	LA/TA = 14/5; LA = 2; 4; 6; 7	19.32	2D C/SiC	Temperature: ↓ 30.4%; specific milling energy: ≈ ↓ 33.3%; S_a: ≈↓ 28.6%
Xie et al. [133]	1D longitudinal	2; 4; 6; 8; 10	23.98	2.5D C/SiC	F_x: ↓ 27%; F_y: ↓ 49.5%; F_z: ↓ 28.6%; S_a: ↓ 53%
Geng et al. [134]	Double bending	9.6	20.73	CFRP	F_x: ↓ 8%–27%; F_y: ↓ 12%–43%; F_z: ↓ 2%–40%; surface roughness: ↓ 54%
Shu et al. [135]	1D longitudinal	10	30	C/C	Fiber pull-out length: ↓ 10%–50%
Zhang et al. [136]	1D longitudinal	15	21.5	C/SiC	–
Islam et al. [137]	1D longitudinal	–	17	C/SiC	–
Liang et al. [138]	1D longitudinal	5	20–30	MD-CFRP	–
Li et al. [139]	1D longitudinal	–	26.5	2.5D SiO_2/SiO_2	Grinding forces: ↓ 30%–35%; S_q: ↓ 12.5%; maximum height of 2D profile S_z: ↓ 12.3%
Wang et al. [140]	1D longitudinal	4	21.2	C/SiC	Grinding forces: ≈ ↓ max 60%
Wang et al. [141]	Vertical; vertical–horizontal	4; 6	–	CFRP	Vertical vibration: F_x: ↓ 11%–20%; F_z: ↓ 12%–40%; S_a: ↓ 12%–21%. Vertical–horizontal vibration: F_x: ↓ 21%–57%; F_z: ↓ 30%–52%; S_a: ↓ 50%–60%
Azarhoushang and Tawakoli [142]	1D tangential	8	20	C/SiC	Grinding forces: ≈ ↓ max 20%; surface roughness R_a and R_z : ≈ ↓ max 30%; G-ratio: ≈ ↑ 30%–40%; radial wear: ≈ ↓ max 28%–45%
Chen et al. [143]	1D longitudinal	14	29.7	CFRP	–
Liang et al. [144]	1D longitudinal	4	26	UD-CFRP	F_t: ↓ max 19% at 135°; F_n: ↓ max 7.2% at 135°; maximum fiber chip length: ≈ ↓ 66%–78%; S_a: ↓ max 17.7%

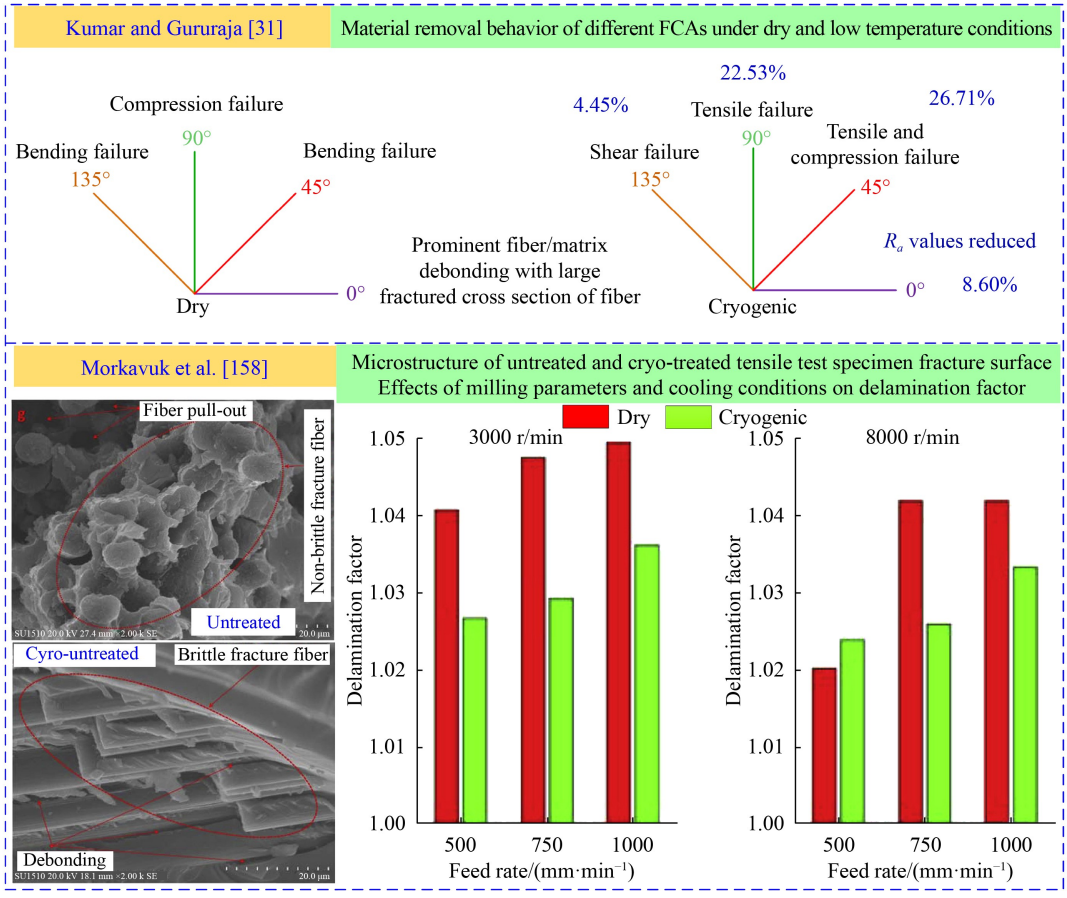

Fig. 9 Mechanisms and advantages of cryogenic cooling in the machining of fiber-reinforced composites. Reproduced with permission from Refs. [31,158] from Elsevier.

conditions on material removal and surface formation mechanism were summarized as follows: (1) The temperature reduction avoids the thermal softening of matrix, which improves the fiber matrix interface strength; (2) the fracture properties of fibers were improved at low temperature. Muhamad Khairussaleh et al. [157] showed that cemented carbide tools experience abrasive wear in CFRP milling whether in dry or cryogenic machining, and the abrasive wear is affected by wear debris and fiber. This abrasive wear is more serious in dry machining because of the generated heat. Therefore, chilled air has the potential to improve the cutting performance of integral cemented carbide tools. El-Hofy et al. [61] used chilled air to minimize thermal damage (bonding and resin melt), and removed workpiece debris and cooling more effectively to prevent burns. Wavy surfaces were observed in the 45° direction, whereas matrix cracking and fiber pullout were suffered because of the high cutting force and resin softening in the 90° and 135° directions. Morkavuk et al. [158] proposed a new cryogenic cooling machining method that immersed the workpiece in cryogenic LN_2 for slot milling of CFRP. The results showed the combination of different damage modes, such as fiber peeling, micro matrix crack, fiber drawing, bundle drawing, delamination, and fiber fracture. Cryogenic cooling machining can reduce the formation of damage but increase the cutting force, because the tensile strength and elastic modulus of CFRPs treated at low temperature are increased by 3.65% and 3.04%, respectively. Cryogenic cooling makes the structure of the workpiece brittle, prevents the thermal damage of the machined surface, improves the fragility of the chip, and reduces the peeling factor, surface roughness, and delamination damage (Fig. 9 [158]). Ohashi et al. [159] believed that liquid nitrogen had a certain effect on preventing delamination, but its grinding force was greater than dry grinding, because solidification increased the hardness of CFRP. The bending strength of CFRP was improved by providing water-soluble coolant and liquid nitrogen during grinding. However, liquid nitrogen cannot obtain the cooling effect similar to flood grinding [160]. Although it is cooled by liquid nitrogen, the grinding temperature in the contact area of the grinding wheel is high because of the increase in workpiece hardness and resistance. Table 2 [31,61,150–158,161,162] lists the temperature conditions under different cryogenic medium modes and their comparison with dry processing results.

Table 2 Cryogenic cooling conditions and output parameters

Reference	Cryogenic medium	Temperature/°C		Composites	Output parameters (compared with dry)
		Supplied	Machined		
Kumar and Gururaja [31]	LN_2	–	44.6	CFRP	Temperature: ↓ 68.9%; damage factor: ≈ ↓ max 10.6%; R_a: ↓ 8.60%, ↓ 26.71%, ↓ 22.53%, and ↓ 4.45%, for 0°, 45°, 90°, and 135°, respectively
El-Hofy et al. [61]	Chilled air of vortex tube	8	–	CFRP	–
Jia et al. [150]	LN_2	–170	–34.4–135.4	CFRP	–
Zhang et al. [151]	LN_2	–	–	SiC/SiC	S_a: ↓ 13% and 22.4% for CVD and PCD tool, respectively
Nor Khairusshima et al. [152]	Chilled air of vortex tube	–10	52	CFRP	Tool life: ↑ 45.6%; R_a: ↓ 16.6%
Nor Khairusshima and Sharifah [153]	Chilled air of vortex tube	–10	–	CFRP	Tool life: ↑ 29.6%
Danish et al. [154]	LN_2; CO_2-snow	–196; –78	100–125; 65–85	CFRP	–
Zou et al. [155]	Supercritical CO_2	–76	34.5	CFRP	S_a: ≈ ↓ max 45.4%; damage factor: ≈ ↓ max 53%; temperature: ↓ 62.9%
Zou et al. [156]	Supercritical CO_2	–70	40–75	CFRP	Temperature: ↓ 58.5%; S_a: ↓ 42.2%
Muhamad Khairussaleh et al. [157]	Chilled air of vortex tube	–10	51.2	CFRP	Temperature: ↓ 49%
Morkavuk et al. [158]	LN_2	–49.9	20.6–23.1	CFRP	Cutting force: ≈ ↑ 45%; surface roughness: ≈ ↓ 23%; tensile strength: ↓ 3.65%; elastic modulus: ↓ 3.04%
F. Wang and Y. Wang [161]	LN_2	–190	–	Quartz-reinforced polyimide composite (QRPC)	–
Cococcetta et al. [162]	LN_2	–198	–	CFRP	Slot milling: linear tool wear: ↓ 60%; tool wear area: ↑ 43%. Edge milling: linear tool wear: ↓ 62%; tool wear area: ↓ 27%

4.3 Minimum quantity lubrication

The hygroscopicity of resin matrix will lead to the water absorption and expansion of CFRP composites, seriously affects its mechanical properties [163–165] which limits the application of casting cooling lubrication in the grinding of CFRP composites. Therefore, most of them currently adopt dry processing. However, the dry machining of CFRP composites usually leads to surface quality deterioration, dust pollution [166], wheel blockage, and various damages (e.g., fiber pull-out, fiber fracture, resin coating, interface cracking, fiber matrix debonding, and delamination). In dry grinding, the grinding temperature in the contact area of the grinding wheel is higher than the thermal substitution temperature of the matrix resin, and the thermal deformation of the matrix resin destroys the grinding surface [91]. Lubricating and cooling medium is the key factor that affects the processing result parameters [154,167]. Some researchers [168,169] have verified the unique advantages of MQL in cutting fiber composites. MQL is a new cooling and lubrication technology [170–172]. High-pressure gas and minimal lubricating oil are mixed and atomized to form oil mist containing droplets, which are sprayed to the cutting area at high speed through the nozzle [173–176]. Given the volatile property of MQL, it has no residue on the wall holes, which avoid the secondary cleaning of aviation parts after processing. MQL liquid forms lubricating oil film on the interface between the tool and workpiece, and high-pressure air mainly plays the role of cooling and chip removal [177–179]. To realize green production from the source of machining, vegetable oil with high biodegradability and nontoxic is generally selected as the base oil [180,181]. This approach greatly reduces the harm of cutting fluid to the environment and human body [182]. Yang et al. [183,184] proved through experiments that MQL could solve the bottleneck of debris formation mechanism in the process of plastic removal of hard and brittle materials. The jet-flow condition of MQL has significant influence on the atomization effect and processing performance [185]. Cococcetta et al. [186] showed that milling CFRP at a lower feed rate would lead to material adhesion to the tool, which leads to tool upsetting material rather than shearing material. MQL reduces the friction and tool wear between the tool tip and the workpiece. Dry machining results in a large number of burrs, which can be reduced significantly by MQL. Qu et al. [30] studied the effect of MQL on the grinding properties of unidirectional C/SiC composites. The

grinding surface quality is optimal, and the grinding force is small when the nozzle angle is 15°, the air pressure is 5 bar (1 bar = 10^5 Pa), the flow rate is 100 mL/h, and the nozzle distance is 80 mm. Smooth fiber separation, fiber fracture, fiber outcrop, fiber pullout, and matrix crack are the main failure forms of the surface. In MQL grinding, water vapor takes away a lot of heat and reduces the grinding temperature significantly. An effective oil film is also formed in the contact area between the grains and the workpiece surface. The experimental results in Esmaeili et al. [187] showed that brittle fracture was the main material removal mechanism of MQL grinding of C/SiC composites. MQL can reduce the cutting force by 37.95%, reduce the surface roughness by 75.93%, and improve the grinding efficiency by 150% compared with dry grinding. The lubrication mechanism of MQL is analyzed, that is, the pressurized directional transportation of oil mist makes oil droplets that penetrate into the pore network on the workpiece and grinding wheel effectively. The G-ratio of MQL grinding is 115.38% higher than that of dry grinding [188]. Pervaiz et al. [189] found different rules and believed that the MQL strategy in external configuration could not provide favorable performance. One possible reason is that part of the lubricant flows into the cavity during MQL-assisted CFRP machining, which leads to the formation of insufficient lubricating film. Through the CFRP milling experiment, Iskandar et al. [190] found that the spray mode that combined high air flow and low oil flow promoted the breakup mechanism of droplets, and the best spray effect was obtained. It also produces a more coherent jet with less vortex formation and better penetration into the cutting area. Finally, the flank wear of MQL is reduced by 30% compared with pressurized air and 22% compared with dry and flood. Although MQL has been proved to have certain potential and advantages in machining of fiber composites, some studies also have different opinions. Helmy et al. [191] found that MQL spray cooling increased cutting force compared with flood, because it did not adequately remove heat and dust in the cutting area. However, MQL has the advantage of reducing the pollution of cooling lubricant and the ability to provide the machining effect when it is close to the requirements of dry machining.

To further improve the heat transfer capacity and tribological characteristics of MQL, some scholars have proposed a new clean cooling and lubrication technology with low carbon, low consumption, and high efficiency nanofluid MQL (NMQL) [192–194]. The technical approach aims to add one or several nanoparticles with different physical and chemical properties to MQL base oil and fully disperse and mix the nanoparticles to prepare nanofluid [195–198]. Then, under the action of high-pressure air flow, the nanofluid is atomized and sprayed into the cutting area through the nozzle [199,200]. NMQL effectively improves the heat transfer capacity and lubrication performance of MQL in the grinding area [201–203]. Some studies show that NMQL achieves a cooling effect close to flood lubrication. In addition, nanoparticles help improve the lubrication characteristics of grinding wheel/workpiece and grain/chip interface because of their excellent anti-wear and antifriction properties [204–206]. Gao et al. [207–209] studied the grinding of CFRP with CNTs nanofluid. Compared with dry grinding, the results show that CNT nano-lubricant reduced maximum F_n and F_t by 20.07% and 26.81%, respectively. The friction coefficient under CNT nano-lubricant MQL is the smallest at $\mu = 0.141$. As shown in Fig. 10 [100,187,208], the grinding force reduction mechanism is explained in two points: (1) The strong constraint of the matrix material on the fiber under temperature reduction is conducive to the removal of fiber by grains; and (2) the excellent tribological properties of CNT nanoparticles at the interface between grains and fiber. The 2D and 3D surface roughness and fractal dimension under NMQL are the lowest. In terms of local morphology characteristics, the spectral width and spectral difference of multi-fractal spectrum of CNTs NMQL are reduced by 21.76% and 31%, respectively, compared with dry grinding. CNT NMQL significantly reduces resin coating, multi-fiber block pull-out, voids, and edge collapse. The nanoparticles filled in the debonding gap between the fiber and the matrix play a supporting role on the fiber, thereby easily removing the fiber (Fig. 10). The oil film between the grinding wheel and workpiece interface can effectively reduce or prevent the adhesion and blockage of resin matrix to grains and effectively improve the blockage of the grinding wheel. Qu et al. [100] carried out the grinding experiment of unidirectional carbon fiber-reinforced CMCs under different conditions, and the results are shown in Fig. 10. In conclusion, the optimal parameters of carbon nanofluid MQL are: nanoparticle concentration of 5 g/L, air pressure of 7 bar, flow rate of 80 mL/h, and nozzle distance of 60 mm. The debonding depth between matrix and carbon fiber depends on the sharpness and lubrication state of grains. James and Nejadian [210] compared the cutting performance of vegetable oil-based NMQL with different nanoparticles (e.g., CNT, Al_2O_3, Ni, and Al) to process different CFRP stacks. The experimental results showed that 2.5%vol Al_2O_3 + MQL reduces the surface roughness of CFRP and titanium composites most than dry machining. However, 1%vol SWCNT + MQL has the optimal effect on improving the surface roughness of CFRP and Al composites. Table 3 [30,100,154,156,162,187,188,191,207,208,210,211] lists the processing results of different MQL conditions and dry processing.

4.4 Tool geometry and coatings

Tool optimization design is one of the main methods used to improve machining quality [212]. In the case of

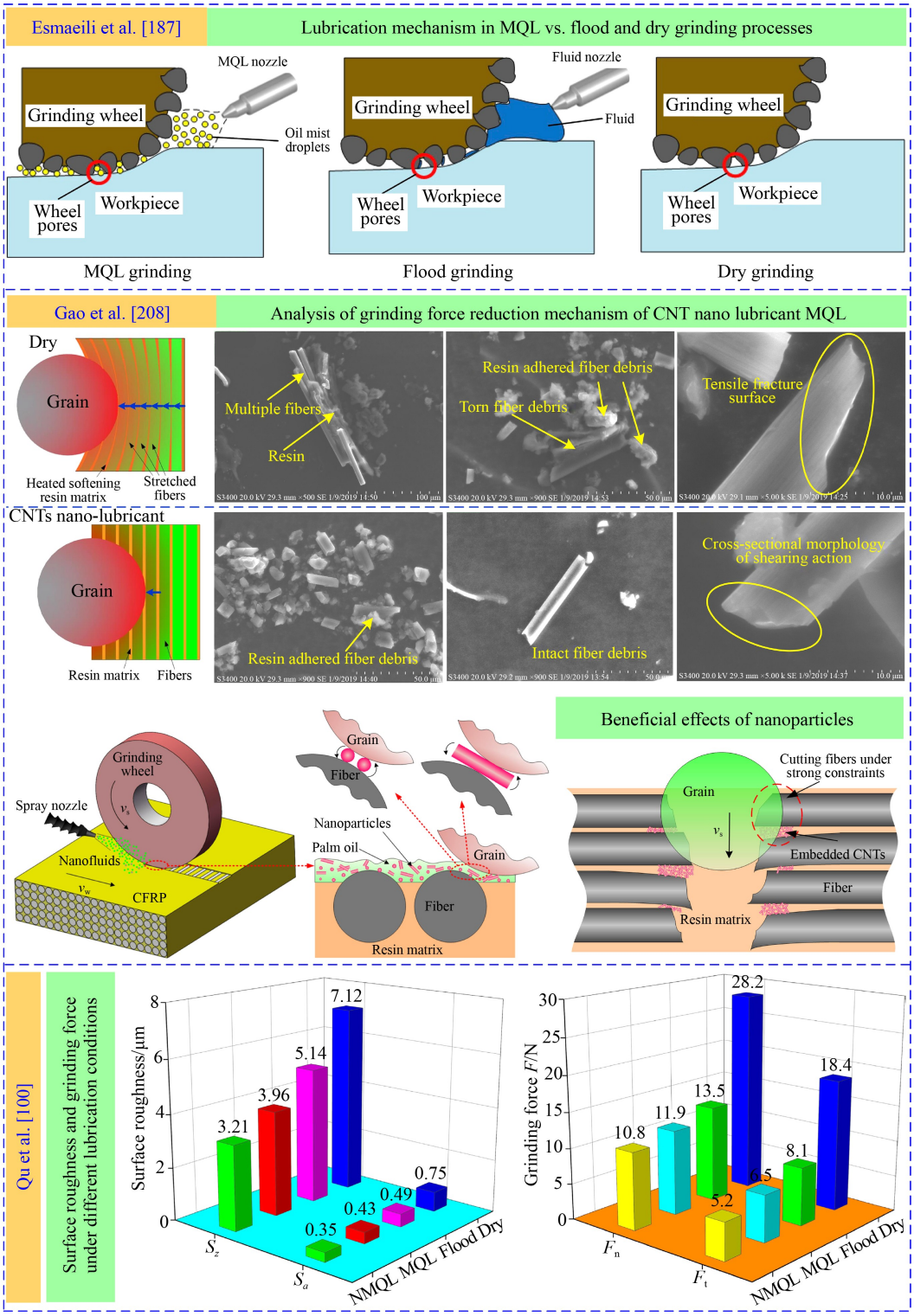

Fig. 10 Lubrication mechanism, force reduction mechanism, and beneficial effects of MQL and NMQL. Reproduced with permission from Refs. [100,187,208] from Elsevier.

fiber-reinforced composites, the geometrical parameters of machining tools have a significant impact on the quality of machined surface (e.g., delamination, fiber pullout, characteristics of uncut fibers, surface roughness, and microstructures). Figure 11 [138,213–217] shows several tool optimization designs for the milling and grinding of fiber-reinforced composites. Wang et al. [213] established a 2D cutting model based on contact of tool/composites and fiber-polymer interface crack analysis. The model proved that inward cutting direction

Table 3 MQL conditions and output parameters

Reference	Lubricant	Supply parameters			Composites	Output parameters (compared with dry)
		Flow rate/(mL·h^{-1})	Air pressure/bar	Device		
Qu et al. [30]	MQL oil	80, 100, 120	3, 5, 7	KINS KS-2107	C/SiC	F_n: ↓ 57.8%; F_t: ↓ 64.7%; S_a: ≈ ↓ 41.3%; S_z: ≈ ↓ 42.9%
Qu et al. [100]	Deionized water-based carbon nanofluid	40, 60, 80, 100	3, 5, 7, 9	KINS KS-2107	C/SiC	F_n: ↓ 62.5%; F_t: ↓ 71.7%; S_a: ≈ ↓ 53.3%; S_z: ≈ ↓ 54.9%
Danish et al. [154]	Eco-friendly MQL oil	150	6	–	CFRP	Friction coefficient: ≈ ↓ 60%
Zou et al. [156]	Cryogenic MQL: soluble vegetable oil	20	85–90	–	CFRP	Temperature: ↓ 70.3%
Cococcetta et al. [162]	Coolube® 2210 oil-based cutting fluid	–	–	UNIST MQL system	CFRP	Slot milling: linear tool wear: ↓ 44%; tool wear area: ↓ 16%. Edge milling: linear tool wear: ↓ 43%; tool wear area: ↓ 30%
Esmaeili et al. [187]	Corn oil	6000	4	MQL system produced by Royal Dutch	C/SiC	Cutting force: ↓ 37.95%; power: ↓ 38.39%; R_a: ↓ 75.93%; G-ratio: ≈ ↑ 70%
Adibi et al. [188]	Corn oil	6000	4	–	C/SiC	F_n: ↓ 31.16%; F_t: ↓ 38.88%; specific grinding energy: ↓ 41.77%; G-ratio: ≈ ↑ 115.38%; R_a: ↓ 75.26%; radial wheel wear: ≈ ↓ 50%–66.7%; grain flattening wear: ≈ ↓ 93.75%
Helmy et al. [191]	Water-based cutting fluid	Two-nozzle system: 2220	4	NEX FLOW mist cooling system	CFRP	–
Gao et al. [207,208]	Palm oil-based CNTs nanofluids	60	6	KINS KS-2106	CFRP	R_a: ↓ 12.68%–17.7%; R_z: ↓ 20.78%–25.06%; average width of profile micro unevenness RS_m: ↓ 11.43%–25.4%; single grain F_n: ↓ 20.07%; single grain F_t: ↓ 26.81%; friction coefficient: ↓ 54%
James and Nejadian [210]	Mixture of castor oil and jojoba oil; oil mixture is enhanced using CNT, Al_2O_3, Ni, and Al	13097	1.013	–	CFRP	–
Rodriguez et al. [211]	Accu-Lube LB-1000 with chlorinated extreme pressure additives	100	8000	–	CFRP	–

and small cutting force are the key to avoid burr and tear. Thrust is the main force that causes damage. Therefore, a left and right edge milling tool, which realizes the inward cutting of fibers on both sides and effectively inhibits burr, tear, and delamination, is proposed. López et al. [214] introduced the development of CNC milling tool series for high-performance CFRP milling. The new milling tool is composed of a plurality of left and right spiral edges, thereby forming a small pyramid edge along the cutting length. Several substrates and coatings, including titanium aluminium nitride (AlTiN) and novel nano cobalt (naCO) with nano-crystalline structure, were also compared. Changing the contact characteristics of the interface between tool and chip can improve the cutting process, which can be realized by the surface texture of the tool. Therefore, Chen et al. [215] manufactured two surface structures on the rake face of double-edge milling tool: linear grooves parallel and perpendicular to the main cutting edge (Fig. 11). The results show that the surface texture of the rake face has a significant effect on the burr formation. The textured tool with linear groove parallel to the main cutting edge is more effective in reducing burr length and surface tearing. The mechanism of micro texture is that the lining groove on the rake face can change the bending deformation of fiber chips, which is conducive to the shear of fiber chips and reduces the length of burrs. In addition, the surface texture on the rake face can store fiber debris and prevent them from slipping on the rake face of the tool. UVAG is an effective method for improving the machining integrity of fiber-reinforced composites. However, serious blockage, rapid tool wear, and poor surface quality are still major problems in the industry because of high heat resistance, wear resistance, and powdery chips of some fiber composites. In conventional grinding, only part of the grains on the grinding wheel play the role of cutting, and other grains generate heat by rubbing the workpiece. The grinding wheel is easily blocked because the grinding wheel with fine grinding particle size does not have enough chip clearance. Yuan et al. [218] proposed a new type of controllable abrasive cluster electroplated grinding wheel.

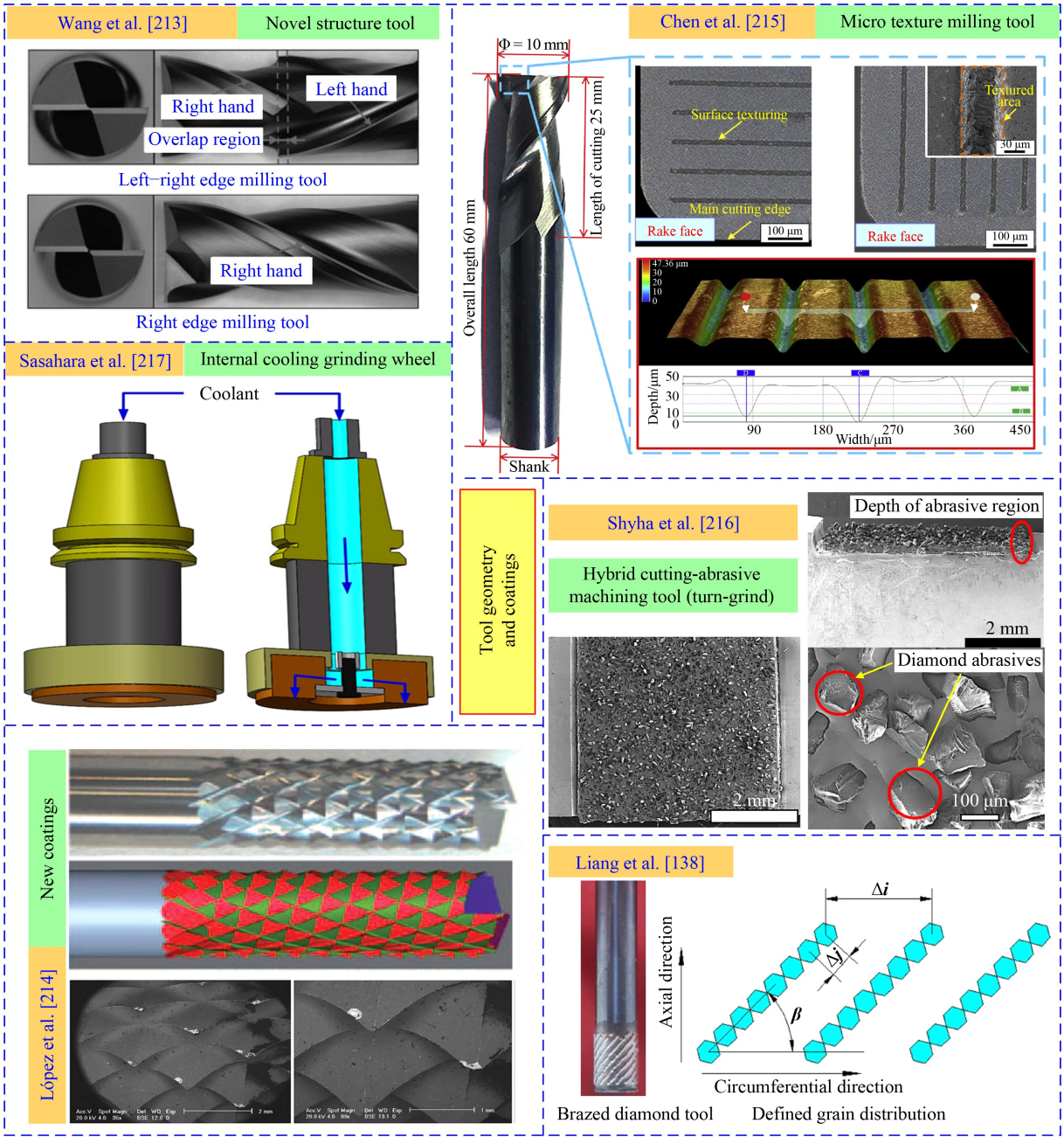

Fig. 11 Typical optimization design of milling and grinding tools. Reproduced with permission from Refs. [138,213–217] from Springer Nature, SAGE Publications, and Elsevier.

Compared with the traditional electroplated grinding wheel, the abrasive on the working surface of the controllable abrasive cluster electroplated grinding wheel is reduced by 81.4%, and the grinding temperature is greatly reduced by nearly 45%, which avoids wheel loading effectively. The space between abrasive clusters is conducive to the removal of grinding chips from the grinding contact area. Shyha et al. [216] developed a new hybrid cutting-abrasive machining tool (turn-grind) for the high-quality machining of fiber-reinforced composites. As shown in Fig. 11, the new tool includes a single point cemented carbide blade and multi-layer diamond abrasive plated to form an abrasive area adjacent to an abrasive free cutting edge [216]. Compared with pure cutting tools, the new cutting abrasive tools reduce the resultant force by 50%; reduce defects, such as delamination and fiber pulling out; and exhibit finer grinding swarf in the chips. To achieve a high-performance machining of fiber composites, Sasahara et al. [217] studied the grinding effect of cup grinding wheel that provided internal coolant on the surface of carbon fiber composites. Internal coolant reduces

grinding force and grinding temperature significantly compared with dry grinding and using external nozzle to supply coolant. In addition, the internal coolant is conducive to removing debris because the coolant is directly supplied to the grinding point through the small hole on the grinding wheel. Okuyama et al. [219] developed a particle arrangement diamond grinding wheel, which has better grinding performance for CFRP than the traditional grinding wheel. Fiber peeling occurs on the machined surface when the FCA is parallel to the cutting direction of the diamond particles. Peeling is effectively reduced when the fiber direction rotates 30°–90° on the horizontal plane. Liang et al. [138] designed a single-layer brazed diamond grinding tool with definite grain distribution. The results show that the grinding force is closely related to the grain row spacing. The grinding force reaches the maximum when the grain row spacing is 1.2 mm. However, the surface roughness is better more active grains and interaction overlapping areas exist. The heat generated during grinding is still a considerable problem because it is significantly higher than the temperature of conventional cutting. Handa and Sooraj [220] introduced a new eccentric sleeve grinding method. The method adopts intermittent progressive cutting strategy to minimize the machining defects of fiber composites. The configuration of eccentric sleeve grinding established an eccentric grinding wheel rotation with cutting and non-cutting zones for abrasive grains, creating a step-by-step cutting scheme without severe fiber-matrix fracture or fiber pull-out. Compared with conventional surface grinding, the grinding force and surface roughness of eccentric sleeve grinding are reduced significantly in the cutting depth range of 20–100 μm.

5 Conclusions and future challenges

5.1 Summary and evaluation

(1) Milling delamination can be divided into interlayer and surface delamination. Compared with interlayer delamination, delamination easily occurs on the surface layer because the surface fiber lacks sufficient matrix supporting force. The milling tool produced an axial milling force F_z on the material because of its spiral angle, which has an upward pushing effect on the surface fiber that results in cracks between layers when F_z is greater than the bonding force between the fiber and the matrix. Furthermore, the cracks will gradually expand and cause delamination. Compared with unidirectional fiber-reinforced composites, the inter-laminar effect of multi-directional composites with different fiber angles between adjacent layers enhances the inter-laminar support provided by adjacent layers.

(2) The delamination of the surface layer is the cause of tearing and burr. The fiber is separated from the matrix after delamination, and some fibers with surface delamination are not completely cut off but are bent and deformed. The fiber elastic deformation recovers and forms burr defects after the milling tool leaves. The suspended fiber would be stirred in by the milling tool with the tool feed, which will pull the fiber, when the residual burr is too long. The fiber root breaks when the tensile force is greater than tensile strength, thereby resulting in tearing defects. In other words, burr and tear refer to the further expansion of delamination defects and the macro embodiment of surface delamination.

(3) The main failure modes of fiber composites in grinding include fiber fracture, matrix fracture or crack, and interface debonding. Brittle fracture mode is the main material removal mechanism of fiber composite grinding. FCA and grain shape play key roles in the formation and morphology of wear debris. Increasing the grinding speed is conducive to the complete removal of fiber, reduces fiber residue and matrix smearing, and improves surface finish and material removal rate. The fiber condition has a greater influence on the processing results than the matrix. The grinding force of fiber composites is also highly dependent on the fiber orientation. The reasons for the difference of grinding force in different grinding directions are discussed.

(4) UVAM has a significant effect on reducing cutting force. The ultrasonic vibration-assisted milling and grinding force models of different fiber composites are discussed. The damage suppression mechanism of UVAM is revealed. UVAG promotes the removal of nano brittle fracture of fibers by reducing the maximum undeformed chip thickness to improve the machined surface quality. The continuous impact of high-frequency and low-amplitude ultrasonic vibration can increase the surface residual compressive stress. The existence of residual compressive stress inhibits the interface crack and hinders the propagation of fiber crack. In addition, ultrasonic vibration changes FCA and promotes transformation from shear fracture mode to dominant fracture mechanism. The effects of different ultrasonic vibration application methods on material removal and damage suppression are summarized. The effects of ultrasonic vibration parameters on machining results are compared. Ultrasonic vibration shows the greatest advantage of restraining machining force, which can be reduced by approximately 60% compared with conventional machining. Ultrasonic vibration can also reduce the surface roughness by about 30%–40% in most cases.

(5) Appropriate machining temperature is the key to ensure the machined surface quality of fiber composites. Satisfactory damage reduction was achieved in cryogenic milling and grinding. The composite is easily extruded and broken because the cryogenic cooling hardening matrix provides stronger support for the fiber. Another reason is that cryogenic reduces tool wear and maintains excellent cutting performance. However, extremely

low-temperature condition causes a sharp increase in cutting force and reduces tool life. Cryogenic cooling is the most effective method for reducing temperature with a maximum reduction of approximately 60%, and the tool wear can be reduced by about 30%–60%. However, it will increase the cutting force by about 40%–50%.

(6) Lubricating cooling medium is also a key factor that affects the machining quality of composites. The hygroscopicity of some specific matrix materials leads to the reduction of mechanical properties, which limits the use of cast lubrication. Therefore, MQL, as a low consumption and clean lubrication–cooling method, has proved to have unique advantages in fiber-reinforced composite cutting. MQL forms an effective oil film in the contact area between the tool and the material surface, which can reduce temperature, friction, tool wear, surface roughness, and burr formation. NMQL is an upgraded technology of MQL that shows better processing effect. MQL can reduce cutting force by approximately 20%–70%, surface roughness by about 10%–70%, and tool wear by about 20%–90%.

(7) The issue of tool design optimization, as an important damage suppression strategy, is discussed. In milling, extensive research focuses on the modification of milling tool geometry modification and coating. As for grinding, the design of grinding wheel mainly includes the arrangement of abrasive particles or clusters. However, the innovative design of tool geometry is mostly based on experience and practice, rather than reasonable theoretical standards. Revealing the machining damage mechanism of fiber-reinforced composites is the basis and key of tool active design.

5.2 Research gap and future trend

(1) Research on the integrated manufacturing of fiber-reinforced composite design, preparation, machines, and performance evaluation for special performance requirements is scarce. Fiber-reinforced composites have excellent designability of multi-phase materials and ply structure, and their damping characteristics are superior to traditional materials. The vibration transmission characteristics of different structural composites vary. The transmission path of vibration in fiber-reinforced composites can be controlled by active design. Therefore, the design and manufacture of composite materials for shock absorption and noise reduction is a hot development direction in the future. This research direction needs to consider the dual performance requirements of vibration reduction effect and machining quality in the machining process systematically.

(2) The high-frequency impact of cutting tools in ultrasonic vibration machining has different effects on materials. The special material parameters, such as the proportion, morphology, arrangement form, and bonding interface of matrix and reinforcement directly affect the removal mode of materials because of the heterogeneity and anisotropy of composites. As a result, the interaction between tool and material in dynamic machining becomes more complex. Therefore, determining the relationship between process parameters and material removal mode in ultrasonic vibration machining, as well as the judgment criteria of material removal mode, which cannot realize the judgment and control of material removal mode, is difficult. The mechanical and thermal stress transfer mechanisms of heterogeneous and anisotropic fiber composites under ultrasonic-assisted machining are unclear. Therefore, integrating the cutting force models under different material removal modes to establish a universe cutting force model is difficult.

(3) At present, the relationship among the material removal mechanism, deformation behavior, and surface formation of fiber composites is far from clear. Thus, the characteristics of deformation, the formation mechanism of wear debris, the formation mechanism of machining performance, and its influencing factors based on the micro and nano scale mechanical properties of the composites must be revealed further. Based on the micro/nano scale composition and mechanical properties of composites, the formation mechanism of subsurface damage, including crack and residual stresses, and the evolution law of material service function, life, and reliability, are investigated. To form a comprehensive evaluation method of the surface/sub surface integrity of composite precision grinding, the effect of thermal mechanical coupling on the mechanical properties of the internal interface of composites must be revealed. To establish the mechanical constitutive model and cross scale material removal model of composites at micro and nano scales further, the mechanical behavior of material removal and the formation process of machined surface must be clarified to provide a systematic and complete theoretical basis for the research of composite processing. Finally, the control of surface/subsurface integrity of composites guided by service performance is realized.

Nomenclature

2D	Two-dimensional
CBN	Cubic boron nitride
CFRP	Carbon fiber reinforced polymer
CG	Conventional grinding
CM	Conventional machining
CMC	Ceramic matrix composite
FCA	Fiber cutting angle
FRP	Fiber reinforced polymer
GFRP	Glass fiber-reinforced plastic
LA	Longitudinal amplitude
LN_2	Liquid nitrogen

MD-CFRP	Multi-directional CFRP
MQL	Minimum quantity lubrication
NMQL	Nanofluid minimum quantity lubrication
QRPC	Quartz-reinforced polyimide composite
SiC	Silicon carbide
SiO_2	Silicon dioxide
SiO_2/SiO_2	Quartz fiber-reinforced silicon dioxide ceramic matrix composite
TA	Torsional amplitude
UD-CFRP	Unidirectional CFRP
UVAG	Ultrasonic vibration-assisted grinding
UVAM	Ultrasonic vibration-assisted machining
UVAS	Ultrasonic vibration-assisted scratching
F_n	Normal force
F_t	Tangential force
F_x	Force in the feeding direction
F_y	Force in the vertical feed direction
F_z	Force in the axial direction
h_{max}	Maximum undeformed chip thickness
R_a	Arithmetical mean deviation of the profile
R_z	Maximum height of the profile
R_t	Distance between the highest and lowest points of the contour
RS_m	Average width of profile micro unevenness
S_a	Arithmetical mean deviation of regional morphology
S_q	Standard deviation of height of each point in the area
S_z	Maximum height of 2D profile
μ	Friction coefficient
$\perp$	Perpendicular to the fiber-bundle axis
$\parallel$	Parallel to the fiber-bundle axis
$\odot$	On the plane normal to the fiber-bundle axis

Acknowledgement This research was financially supported by the National Key R&D Program of China (Grant No. 2020YFB2010500), the National Natural Science Foundation of China (Grant Nos. 51975305 and 51905289), Shandong Natural Science Foundation, China (Grant Nos. ZR2020KE027 and ZR2020ME158), the Innovation Talent Supporting Program for Postdoctoral Fellows of Shandong Province, China (Grant No. SDBX2020012), and the Major Science and Technology Innovation Engineering Projects of Shandong Province, China (Grant No. 2019JZZY020111).

References

1. Rao G V G, Mahajan P, Bhatnagar N. Three-dimensional macro-mechanical finite element model for machining of unidirectional-fiber reinforced polymer composites. Materials Science and Engineering A, 2008, 498(1–2): 142–149
2. Niu B, Li S J, Yang R. Manufacturing and mechanical properties of composite orthotropic Kagome honeycomb using novel modular method. Frontiers of Mechanical Engineering, 2020, 15(3): 484–495
3. Wang B, Zhao F, Zhao Z X, Xu K P. Influence factors on natural frequencies of composite materials. Frontiers of Mechanical Engineering, 2020, 15(4): 571–584
4. Henerichs M, Voß R, Kuster F, Wegener K. Machining of carbon fiber reinforced plastics: influence of tool geometry and fiber orientation on the machining forces. CIRP Journal of Manufacturing Science and Technology, 2015, 9: 136–145
5. Bai J B, Bu G Y. Progress in 4D printing technology. Journal of Advanced Manufacturing Science and Technology, 2022, 2(1): 2022001
6. Gao T, Li C H, Wang Y Q, Liu X S, An Q L, Li H N, Zhang Y B, Cao H J, Liu B, Wang D Z, Said Z, Debnath S, Jamil M, Ali H M, Sharma S. Carbon fiber reinforced polymer in drilling: from damage mechanisms to suppression. Composite Structures, 2022, 286: 115232
7. Rajasekaran T, Palanikumar K, Vinayagam B K. Experimental investigation and analysis in turning of CFRP composites. Journal of Composite Materials, 2012, 46(7): 809–821
8. Abhishek K, Kumar V R, Datta S, Mahapatra S S. Application of JAYA algorithm for the optimization of machining performance characteristics during the turning of CFRP (epoxy) composites: comparison with TLBO, GA, and ICA. Engineering with Computers, 2017, 33(3): 457–475
9. Hosokawa A, Hirose N, Ueda T, Furumoto T. High-quality machining of CFRP with high helix end mill. CIRP Annals, 2014, 63(1): 89–92
10. Voss R, Seeholzer L, Kuster F, Wegener K. Influence of fibre orientation, tool geometry and process parameters on surface quality in milling of CFRP. CIRP Journal of Manufacturing Science and Technology, 2017, 18: 75–91
11. Geng D X, Liu Y H, Shao Z Y, Lu Z H, Cai J, Li X, Jiang X G, Zhang D Y. Delamination formation, evaluation and suppression during drilling of composite laminates: a review. Composite Structures, 2019, 216: 168–186
12. Geier N, Davim J P, Szalay T. Advanced cutting tools and technologies for drilling carbon fibre reinforced polymer (CFRP) composites: a review. Composites Part A: Applied Science and Manufacturing, 2019, 125: 105552
13. Wang H, Hu Y B, Cong W L, Hu Z L. A mechanistic model on feeding-directional cutting force in surface grinding of CFRP composites using rotary ultrasonic machining with horizontal

ultrasonic vibration. International Journal of Mechanical Sciences, 2019, 155: 450–460

14. Kim P J, Lee D G, Choi J K. Grinding characteristics of carbon fiber epoxy composite hollow shafts. Journal of Composite Materials, 2000, 34(23): 2016–2035
15. Huang B T, Li C H, Zhang Y B, Ding W F, Yang M, Yang Y Y, Zhai H, Xu X F, Wang D Z, Debnath S, Jamil M, Li H N, Ali H M, Gupta M K, Said Z. Advances in fabrication of ceramic corundum abrasives based on sol-gel process. Chinese Journal of Aeronautics, 2021, 34(6): 1–17
16. Niu J B, Xu J T, Ren F, Sun Y W, Guo D M. A short review on milling dynamics in low-stiffness cutting conditions: modeling and analysis. Journal of Advanced Manufacturing Science and Technology, 2021, 1(1): 2020004
17. Xiao G J, Zhang Y D, Huang Y, Song S Y, Chen B Q. Grinding mechanism of titanium alloy: research status and prospect. Journal of Advanced Manufacturing Science and Technology, 2021, 1(1): 2020001
18. Dang X B, Wan M, Yang Y. Prediction and suppression of chatter in milling of structures with low-rigidity: a review. Journal of Advanced Manufacturing Science and Technology, 2021, 1(3): 2021010
19. Yao Z Q, Fan C, Zhang Z, Zhang D H, Luo M. Position-varying surface roughness prediction method considering compensated acceleration in milling of thin-walled workpiece. Frontiers of Mechanical Engineering, 2021, 16(4): 855–867
20. Zhu S W, Xiao G J, He Y, Liu G, Song S Y, Jiahua S L. Tip vortex cavitation of propeller bionic noise reduction surface based on precision abrasive belt grinding. Journal of Advanced Manufacturing Science and Technology, 2022, 2(1): 2022003
21. Huang B T, Zhang Y B, Wang X M, Chen Y, Cao H J, Liu B, Nie X L, Li C H. Experimental evaluation of wear mechanism and grinding performance of SG wheel in machining nickel-based alloy GH4169. Surface Technology, 2021, 50(12): 62–70
22. Xiong Y F, Wang W H, Shi Y Y, Jiang R S, Lin K Y, Song G D, Shao M W, Liu X F, Li J C, Shan C W. Machining performance of *in-situ* TiB_2 particle reinforced Al-based metal matrix composites: a literature review. Journal of Advanced Manufacturing Science and Technology, 2021, 1(2): 2021003
23. Chardon G, Chanal H, Duc E, Garnier T. Study of surface finish of fiber-reinforced composite molds. Proceedings of the Institution of Mechanical Engineers, Part B: Journal of Engineering Manufacture, 2017, 231(4): 576–587
24. Wang H, Sun J, Li J, Li W. Roughness modelling analysis for milling of carbon fibre reinforced polymer composites. Materials Technology, 2015, 30(sup1): A46–A50
25. Garcia Luna G, Axinte D, Novovic D. Influence of grit geometry and fibre orientation on the abrasive material removal mechanisms of SiC/SiC ceramic matrix composites (CMCs). International Journal of Machine Tools and Manufacture, 2020, 157: 103580
26. Yuan J L, Lyu B H, Hang W, Deng Q F. Review on the progress of ultra-precision machining technologies. Frontiers of Mechanical Engineering, 2017, 12(2): 158–180
27. Sen A K, Litak G, Syta A, Rusinek R. Intermittency and multiscale dynamics in milling of fiber reinforced composites. Meccanica, 2013, 48(4): 783–789
28. Antwi E, Liu K, Wang H. A review on ductile mode cutting of brittle materials. Frontiers of Mechanical Engineering, 2018, 13(2): 251–263
29. Mu D F, Liu X L, Yue C X, Liu Q, Bai Z Y, Liang S Y, Ding Y P. On-line tool wear monitoring based on machine learning. Journal of Advanced Manufacturing Science and Technology, 2021, 1(2): 2021002
30. Qu S S, Gong Y D, Yang Y Y, Sun Y, Wen X L, Qi Y. Investigating minimum quantity lubrication in unidirectional C_f/SiC composite grinding. Ceramics International, 2020, 46(3): 3582–3591
31. Kumar D, Gururaja S. Machining damage and surface integrity evaluation during milling of UD-CFRP laminates: dry vs. cryogenic. Composite Structures, 2020, 247: 112504
32. Koplev A, Lystrup A, Vorm T. The cutting process, chips, and cutting forces in machining CFRP. Composites, 1983, 14(4): 371–376
33. Kaneeda T, Takahashi M. CFRP cutting mechanism (1st report): surface generation mechanism at very low cutting speeds. Journal of the Japan Society for Precision Engineering, 1989, 55(8): 1456–1461
34. Arola D, Ramulu M, Wang D H. Chip formation in orthogonal trimming of graphite/epoxy composite. Composites Part A: Applied Science and Manufacturing, 1996, 27(2): 121–133
35. Nayak D, Bhatnagar N, Mahajan P. Machining studies of uni-directional glass fiber reinforced plastic (UD-GFRP) composites part 1: effect of geometrical and process parameters. Machining Science and Technology, 2005, 9(4): 481–501
36. Li H, Qin X D, He G Y, Jin Y, Sun D, Price M. Investigation of chip formation and fracture toughness in orthogonal cutting of UD-CFRP. The International Journal of Advanced Manufacturing Technology, 2016, 82(5–8): 1079–1088
37. Ahmad J. Machining of Polymer Composites. Boston: Springer, 2009
38. Wang D H, Ramulu M, Arola D. Orthogonal cutting mechanisms of graphite/epoxy composite. Part I: unidirectional laminate. International Journal of Machine Tools and Manufacture, 1995, 35(12): 1623–1638
39. Karpat Y, Bahtiyar O, Değer B. Mechanistic force modeling for milling of unidirectional carbon fiber reinforced polymer laminates. International Journal of Machine Tools and Manufacture, 2012, 56: 79–93
40. Liu H T, Lin J, Sun Y Z, Zhang J Y. Micro model of carbon fiber/cyanate ester composites and analysis of machining damage mechanism. Chinese Journal of Mechanical Engineering, 2019, 32(1): 52
41. Ghafarizadeh S, Chatelain J F, Lebrun G. Finite element analysis of surface milling of carbon fiber-reinforced composites. The International Journal of Advanced Manufacturing Technology, 2016, 87(1–4): 399–409
42. Azmi A I. Chip formation studies in machining fibre reinforced polymer composites. International Journal of Materials and Product Technology, 2013, 46(1): 32–46
43. Uysal A, Altan M. Quality during milling of a glass fiber reinforced polymer composite. Materials Testing, 2015, 57(9): 767–772

44. Çelik Y H, Kılıçkap E, Yardımeden A. Estimate of cutting forces and surface roughness in end milling of glass fiber reinforced plastic composites using fuzzy logic system. Science and Engineering of Composite Materials, 2014, 21(3): 435–443
45. Wang F B, Wang Y Q. Milling properties of Kevlar 49 fiber composite based on fiber orientation in cryogenic cooling. The International Journal of Advanced Manufacturing Technology, 2019, 103(9–12): 4609–4619
46. Fu Q, Wu S J, Li C H, Xu J Y, Wang D Z. Delamination and chip breaking mechanism of orthogonal cutting CFRP/Ti6Al4V composite. Journal of Manufacturing Processes, 2022, 73: 183–196
47. Wang F J, Bi G J, Ning F D. Modeling of dynamic milling forces considering the interlaminar effect during milling multidirectional CFRP laminate. Journal of Reinforced Plastics and Composites, 2021, 40(11–12): 437–449
48. Colligan K, Ramulu M. Delamination in surface plies of graphite/epoxy caused by the edge trimming process. In: Proceedings of the Symposium, the 112th ASME Winter Annual Meeting. Atlanta: ASME, 1991, 49(27): 113–125
49. Colligan K, Ramulu M. The effect of edge trimming on composite surface plies. Manufacturing Review, 1992, 5(4): 274–283
50. Sui J B, Wang C Y. Machinability study of unidirectional CFRP laminates by slot milling. The International Journal of Advanced Manufacturing Technology, 2019, 100(1–4): 189–197
51. Ning H F, Zheng H L, Zhang S G, Yuan X M. Milling force prediction model development for CFRP multidirectional laminates and segmented specific cutting energy analysis. The International Journal of Advanced Manufacturing Technology, 2021, 113(9−10): 2437–2445
52. Hintze W, Cordes M, Koerkel G. Influence of weave structure on delamination when milling CFRP. Journal of Materials Processing Technology, 2015, 216: 199–205
53. Sheikh-Ahmad J, Urban N, Cheraghi H. Machining damage in edge trimming of CFRP. Materials and Manufacturing Processes, 2012, 27(7): 802–808
54. Hintze W, Hartmann D, Schütte C. Occurrence and propagation of delamination during the machining of carbon fibre reinforced plastics (CFRPs)—an experimental study. Composites Science and Technology, 2011, 71(15): 1719–1726
55. Hintze W, Hartmann D. Modeling of delamination during milling of unidirectional CFRP. Procedia CIRP, 2013, 8: 444–449
56. Azmi A I, Lin R J T, Bhattacharyya D. Machinability study of glass fibre-reinforced polymer composites during end milling. The International Journal of Advanced Manufacturing Technology, 2013, 64(1–4): 247–261
57. Wang F J, Gu T Y, Wang X N, Jin X H, Zhang B Y. Analysis of burr and tear in milling of carbon fiber reinforced plastic (CFRP) using finite element method. Applied Composite Materials, 2021, 28(4): 991–1018
58. Wang H J, Sun J, Zhang D D, Guo K, Li J F. The effect of cutting temperature in milling of carbon fiber reinforced polymer composites. Composites Part A: Applied Science and Manufacturing, 2016, 91: 380–387
59. He Y L, Qing H A, Zhang S G, Wang D Z, Zhu S W. The cutting force and defect analysis in milling of carbon fiber-reinforced polymer (CFRP) composite. The International Journal of Advanced Manufacturing Technology, 2017, 93(5–8): 1829–1842
60. Liu G J, Chen H Y, Huang Z, Gao F, Chen T. Surface quality of staggered PCD end mill in milling of carbon fiber reinforced plastics. Applied Sciences, 2017, 7(2): 199
61. El-Hofy M H, Soo S L, Aspinwall D K, Sim W M, Pearson D, Harden P. Factors affecting workpiece surface integrity in slotting of CFRP. Procedia Engineering, 2011, 19: 94–99
62. Ghidossi P, El Mansori M, Pierron F. Influence of specimen preparation by machining on the failure of polymer matrix off-axis tensile coupons. Composites Science and Technology, 2006, 66(11–12): 1857–1872
63. Ghidossi P, El Mansori M, Pierron F. Edge machining effects on the failure of polymer matrix composite coupons. Composites Part A: Applied Science and Manufacturing, 2004, 35(78): 989–999
64. Hou Y, Yao P, Zhang H Y, Liu X, Liu H L, Huang C Z, Zhang Z H. Chatter stability and surface quality in milling of unidirectional carbon fiber reinforced polymer. Composite Structures, 2021, 271: 114131
65. Zhang L F, Wang S, Qiao W L, Li Z, Wang N, Zhang J, Wang T. High-speed milling of CFRP composites: a progressive damage model of cutting force. The International Journal of Advanced Manufacturing Technology, 2020, 106(3–4): 1005–1015
66. Qu S S, Yao P, Gong Y D, Yang Y Y, Chu D K, Zhu Q S. Modelling and grinding characteristics of unidirectional C–SiCs. Ceramics International, 2022, 48(6): 8314–8324
67. Hu N S, Zhang L C. A study on the grindability of multidirectional carbon fibre-reinforced plastics. Journal of Materials Processing Technology, 2003, 140(1–3): 152–156
68. Liu Q, Huang G Q, Xu X P, Fang C F, Cui C C. A study on the surface grinding of 2D C/SiC composites. The International Journal of Advanced Manufacturing Technology, 2017, 93(5–8): 1595–1603
69. Yin J F, Xu J H, Ding W F, Su H H. Effects of grinding speed on the material removal mechanism in single grain grinding of SiC_f/SiC ceramic matrix composite. Ceramics International, 2021, 47(9): 12795–12802
70. Qu S S, Gong Y D, Yang Y Y, Xu Y C, Wang W W, Xin B, Pang S Y. Mechanical model and removal mechanism of unidirectional carbon fibre-reinforced ceramic composites. International Journal of Mechanical Sciences, 2020, 173: 105465
71. Zhang L F, Ren C Z, Ji C H, Wang Z Q, Chen G. Effect of fiber orientations on surface grinding process of unidirectional C/SiC composites. Applied Surface Science, 2016, 366: 424–431
72. Yang Y Y, Qu S S, Gong Y D. Investigating the grinding performance of unidirectional and 2.5D-C/SiCs. Ceramics International, 2021, 47(4): 5123–5132
73. Liu Q, Huang G Q, Xu X P, Fang C F, Cui C C. Influence of grinding fiber angles on grinding of the 2D-C_f/C-SiC composites. Ceramics International, 2018, 44(11): 12774–12782
74. Liu Q, Huang G Q, Cui C C, Tong Z, Xu X P. Investigation of grinding mechanism of a 2D C_f/C-SiC composite by single-grain scratching. Ceramics International, 2019, 45(10): 13422–13430
75. Li Y C, Ge X, Wang H, Hu Y B, Ning F D, Cong W L, Ren C Z.

Study of material removal mechanisms in grinding of C/SiC composites via single-abrasive scratch tests. Ceramics International, 2019, 45(4): 4729–4738

76. Wei J H, Wang H J, Lin B, Sui T Y, Zhao F F, Fang S. Acoustic emission signal of fiber-reinforced composite grinding: frequency components and damage pattern recognition. The International Journal of Advanced Manufacturing Technology, 2019, 103(1–4): 1391–1401
77. Wang Y G, Wang H J, Wei J H, Lin B, Xu J Y, Fang S. Finite element analysis of grinding process of long fiber reinforced ceramic matrix woven composites: modeling, experimental verification and material removal mechanism. Ceramics International, 2019, 45(13): 15920–15927
78. Cao J G, Wu Y B, Lu D, Fujimoto M, Nomura M. Material removal behavior in ultrasonic-assisted scratching of SiC ceramics with a single diamond tool. International Journal of Machine Tools and Manufacture, 2014, 79: 49–61
79. Suya Prem Anand P, Arunachalam N, Vijayaraghavan L. Study on grinding of pre-sintered zirconia using diamond wheel. Materials and Manufacturing Processes, 2018, 33(6): 634–643
80. Inoue H, Kawaguchi I. Study on the grinding mechanism of glass fiber reinforced plastics. Journal of Engineering Materials and Technology, 1990, 112(3): 341–345
81. Chockalingam P, Kuang K C, Vijayaram T R. Effects of grinding process parameters and coolants on the grindability of GFRP laminates. Materials and Manufacturing Processes, 2013, 28(10): 1071–1076
82. Chockalingam P, Kuang K C. Effects of abrasive types on grinding of chopped strand mat glass fiber-reinforced polymer composite laminates. Machining Science and Technology, 2015, 19(2): 313–324
83. Wei J H, Wang H J, Lin B, Sui T Y, Zhao F F, Fang S. A force model in single grain grinding of long fiber reinforced woven composite. The International Journal of Advanced Manufacturing Technology, 2019, 100(1–4): 541–552
84. Sambhav K, Kumar A, Choudhury S K. Mechanistic force modeling of single point cutting tool in terms of grinding angles. International Journal of Machine Tools and Manufacture, 2011, 51(10–11): 775–786
85. Sun J L, Qin F, Chen P, An T. A predictive model of grinding force in silicon wafer self-rotating grinding. International Journal of Machine Tools and Manufacture, 2016, 109: 74–86
86. Cao X Y, Lin B, Zhang X F. Investigations on grinding process of woven ceramic matrix composite based on reinforced fiber orientations. Composites Part B: Engineering, 2015, 71: 184–192
87. Zhang L F, Wang S, Li Z, Qiao W L, Wang Y, Wang T. Influence factors on grinding force in surface grinding of unidirectional C/SiC composites. Applied Composite Materials, 2019, 26(3): 1073–1085
88. Chen J Y, Shen J Y, Huang H, Xu X P. Grinding characteristics in high speed grinding of engineering ceramics with brazed diamond wheels. Journal of Materials Processing Technology, 2010, 210(6–7): 899–906
89. Ding K, Fu Y C, Su H H, Xu H X, Cui F F, Li Q L. Experimental studies on matching performance of grinding and vibration parameters in ultrasonic assisted grinding of SiC ceramics. The International Journal of Advanced Manufacturing Technology, 2017, 88(9–12): 2527–2535
90. Liu S L, Chen T, Wu C Q. Rotary ultrasonic face grinding of carbon fiber reinforced plastic (CFRP): a study on cutting force model. The International Journal of Advanced Manufacturing Technology, 2017, 89(1–4): 847–856
91. Kodama H, Okazaki S, Jiang Y F, Yoden H, Ohashi K. Thermal influence on surface layer of carbon fiber reinforced plastic (CFRP) in grinding. Precision Engineering, 2020, 65: 53–63
92. Sheikh-Ahmad J, Mohammed J. Optimization of process parameters in diamond abrasive machining of carbon fiber-reinforced epoxy. Materials and Manufacturing Processes, 2014, 29(11–12): 1361–1366
93. Fan B P, Chen Y, Chen B B, Liang Y H, Sun L. Finite element analysis on heat distribution ratio during grinding CFRP. Diamond and Abrasives Engineering, 2019, 39(1): 66−71 (in Chinese)
94. Sheikh-Ahmad J Y, Almaskari F, Hafeez F, Meng F Y. Evaluation of heat partition in machining CFRP using inverse method. Machining Science and Technology, 2019, 23(4): 530–546
95. Qian M, Xiao J Z, Wang G F, Huang P C, Chen Z Z, Han G R. Evaluation of heat generation using a microscopic cutting model with thermo-mechanical coupling for carbon fiber reinforced polymer composites. Journal of Reinforced Plastics and Composites, 2020, 39(21–22): 793–804
96. Wang H, Cong W L, Ning F D, Hu Y B. A study on the effects of machining variables in surface grinding of CFRP composites using rotary ultrasonic machining. The International Journal of Advanced Manufacturing Technology, 2018, 95(9–12): 3651–3663
97. Choudhary A, Das Chakladar N, Paul S. Identification and estimation of defects in high-speed ground C/SiC ceramic matrix composites. Composite Structures, 2021, 261: 113274
98. Hanasaki S, Fujiwara J. Tashiro T. Study on surface grinding of unidirectional carbon fiber reinforced plastics in dry method. In: Proceedings of International Conference on Leading Edge Manufacturing in 21st Century: LEM21. 2003, 297–302
99. Soo S L, Shyha I S, Barnett T, Aspinwall D K, Sim W M. Grinding performance and workpiece integrity when superabrasive edge routing carbon fibre reinforced plastic (CFRP) composites. CIRP Annals, 2012, 61(1): 295–298
100. Qu S S, Gong Y D, Yang Y Y, Wang W W, Liang C Y, Han B. An investigation of carbon nanofluid minimum quantity lubrication for grinding unidirectional carbon fibre-reinforced ceramic matrix composites. Journal of Cleaner Production, 2020, 249: 119353
101. Cao X Y, Lin B, Zhang X F. A study on grinding surface waviness of woven ceramic matrix composites. Applied Surface Science, 2013, 270: 503–512
102. Gavalda Diaz O, Axinte D A. Towards understanding the cutting and fracture mechanism in ceramic matrix composites. International Journal of Machine Tools and Manufacture, 2017, 118–119: 12–25
103. Cao X Y, Lin B, Wang Y, Wang S L. Influence of diamond wheel grinding process on surface micro-topography and

properties of SiO_2/SiO_2 composite. Applied Surface Science, 2014, 292: 181–189

104. Xu J, Feng P F, Feng F, Zha H T, Liang G Q. Subsurface damage and burr improvements of aramid fiber reinforced plastics by using longitudinal–torsional ultrasonic vibration milling. Journal of Materials Processing Technology, 2021, 297: 117265
105. Yuan S M, Fan H T, Amin M, Zhang C, Guo M. A cutting force prediction dynamic model for side milling of ceramic matrix composites C/SiC based on rotary ultrasonic machining. The International Journal of Advanced Manufacturing Technology, 2016, 86(1–4): 37–48
106. Xu S, Kuriyagawa T, Shimada K, Mizutani M. Recent advances in ultrasonic-assisted machining for the fabrication of micro/nano-textured surfaces. Frontiers of Mechanical Engineering, 2017, 12(1): 33–45
107. Babbar A, Sharma A, Jain V, Jain A K. Rotary ultrasonic milling of C/SiC composites fabricated using chemical vapor infiltration and needling technique. Materials Research Express, 2019, 6(8): 085607
108. Verma G C, Pandey P M. Machining forces in ultrasonic-vibration assisted end milling. Ultrasonics, 2019, 94: 350–363
109. Gao T, Zhang X P, Li C H, Zhang Y B, Yang M, Jia D Z, Ji H J, Zhao Y J, Li R Z, Yao P, Zhu L D. Surface morphology evaluation of multi-angle 2D ultrasonic vibration integrated with nanofluid minimum quantity lubrication grinding. Journal of Manufacturing Processes, 2020, 51: 44–61
110. Wang Y, Sarin V K, Lin B, Li H, Gillard S. Feasibility study of the ultrasonic vibration filing of carbon fiber reinforced silicon carbide composites. International Journal of Machine Tools and Manufacture, 2016, 101: 10–17
111. Ma G F, Kang R K, Dong Z G, Yin S, Bao Y, Guo D M. Hole quality in longitudinal–torsional coupled ultrasonic vibration assisted drilling of carbon fiber reinforced plastics. Frontiers of Mechanical Engineering, 2020, 15(4): 538–546
112. Chen J, An Q L, Ming W W, Chen M. Investigation on machined surface quality in ultrasonic-assisted grinding of C_f/SiC composites based on fracture mechanism of carbon fibers. The International Journal of Advanced Manufacturing Technology, 2020, 109(5–6): 1583–1599
113. Ding K, Fu Y C, Su H H, Cui F F, Li Q L, Lei W N, Xu H X. Study on surface/subsurface breakage in ultrasonic assisted grinding of C/SiC composites. The International Journal of Advanced Manufacturing Technology, 2017, 91(9–12): 3095–3105
114. Ning F D, Wang H, Cong W L. Rotary ultrasonic machining of carbon fiber reinforced plastic composites: a study on fiber material removal mechanism through single-grain scratching. The International Journal of Advanced Manufacturing Technology, 2019, 103(1–4): 1095–1104
115. Xue F, Zheng K, Liao W H, Shu J, Miao D D. Experimental investigation on fatigue property at room temperature of C/SiC composites machined by rotary ultrasonic milling. Journal of the European Ceramic Society, 2021, 41(6): 3341–3356
116. Cong W L, Pei Z J, Mohanty N, Van Vleet E, Treadwell C. Vibration amplitude in rotary ultrasonic machining: a novel measurement method and effects of process variables. Journal of Manufacturing Science and Engineering, 2011, 133(3): 034501
117. Fernando P K S C, Zhang M, Pei Z J. Rotary ultrasonic machining: effects of tool natural frequency on ultrasonic vibration amplitude. Machining Science and Technology, 2019, 23(4): 595–611
118. Xu W X, Zhang L C, Wu Y B. Elliptic vibration-assisted cutting of fibre-reinforced polymer composites: understanding the material removal mechanisms. Composites Science and Technology, 2014, 92: 103–111
119. Yang Z C, Zhu L D, Zhang G X, Ni C B, Lin B. Review of ultrasonic vibration-assisted machining in advanced materials. International Journal of Machine Tools and Manufacture, 2020, 156: 103594
120. Wang H, Hu Y B, Cong W L, Hu Z Y, Wang Y Q. A novel investigation on horizontal and 3D elliptical ultrasonic vibrations in rotary ultrasonic surface machining of carbon fiber reinforced plastic composites. Journal of Manufacturing Processes, 2020, 52: 12–25
121. Wang J J, Zhang J F, Feng P F. Effects of tool vibration on fiber fracture in rotary ultrasonic machining of C/SiC ceramic matrix composites. Composites Part B: Engineering, 2017, 129: 233–242
122. Amin M, Yuan S M, Khan M Z, Zhang C, Wu Q. Development of cutting force prediction model for carbon fiber reinforced polymers based on rotary ultrasonic slot milling. Machining Science and Technology, 2018, 22(3): 402–426
123. Amin M, Yuan S M, Khan M Z, Wu Q, Zhu G Y. Development of a generalized cutting force prediction model for carbon fiber reinforced polymers based on rotary ultrasonic face milling. The International Journal of Advanced Manufacturing Technology, 2017, 93(5–8): 2655–2666
124. Wang H, Pei Z J, Cong W L. A mechanistic cutting force model based on ductile and brittle fracture material removal modes for edge surface grinding of CFRP composites using rotary ultrasonic machining. International Journal of Mechanical Sciences, 2020, 176: 105551
125. Ning F D, Cong W L, Wang H, Hu Y B, Hu Z L, Pei Z J. Surface grinding of CFRP composites with rotary ultrasonic machining: a mechanistic model on cutting force in the feed direction. The International Journal of Advanced Manufacturing Technology, 2017, 92(1–4): 1217–1229
126. Li Y C, Ren C Z, Wang H, Hu Y B, Ning F D, Wang X L, Cong W L. Edge surface grinding of CFRP composites using rotary ultrasonic machining: comparison of two machining methods. The International Journal of Advanced Manufacturing Technology, 2019, 100(9–12): 3237–3248
127. Wang H, Ning F D, Hu Y B, Cong W L. Surface grinding of CFRP composites using rotary ultrasonic machining: a comparison of workpiece machining orientations. The International Journal of Advanced Manufacturing Technology, 2018, 95(5–8): 2917–2930
128. Xue F, Zheng K, Liao W H, Shu J, Dong S. Investigation on fiber fracture mechanism of C/SiC composites by rotary ultrasonic milling. International Journal of Mechanical Sciences, 2021, 191: 106054
129. Amin M, Yuan S M, Israr A, Zhen L, Qi W. Development of cutting force prediction model for vibration-assisted slot milling

of carbon fiber reinforced polymers. The International Journal of Advanced Manufacturing Technology, 2018, 94(9–12): 3863–3874

130. Yuan S M, Zhu G Y, Zhang C. Modeling of tool blockage condition in cutting tool design for rotary ultrasonic machining of composites. The International Journal of Advanced Manufacturing Technology, 2017, 91(5–8): 2645–2654
131. Liu Y, Liu Z B, Wang X B, Huang T. Experimental study on cutting force and surface quality in ultrasonic vibration-assisted milling of C/SiC composites. The International Journal of Advanced Manufacturing Technology, 2021, 112(7–8): 2003–2014
132. Chen J, Ming W W, An Q L, Chen M. Mechanism and feasibility of ultrasonic-assisted milling to improve the machined surface quality of 2D C_f/SiC composites. Ceramics International, 2020, 46(10): 15122–15136
133. Xie Z W, Liu Z Q, Wang B, Xin M Z, Song Q H, Jiang L P. Longitudinal amplitude effect on material removal mechanism of ultrasonic vibration-assisted milling 2.5D C/SiC composites. Ceramics International, 2021, 47(22): 32144–32152
134. Geng D X, Zhang D Y, Xu Y G, He F T, Liu D P, Duan Z H. Rotary ultrasonic elliptical machining for side milling of CFRP: tool performance and surface integrity. Ultrasonics, 2015, 59: 128–137
135. Shu J, Liao W H, Zheng K, Hussein Youssef A M F. Surface morphology on carbon fiber composites by rotary ultrasonic milling. Machining Science and Technology, 2021, 25(5): 721–737
136. Zhang C, Yuan S M, Amin M, Fan H T, Liu Q. Development of a cutting force prediction model based on brittle fracture for C/SiC in rotary ultrasonic facing milling. The International Journal of Advanced Manufacturing Technology, 2016, 85(1–4): 573–583
137. Islam S, Yuan S M, Li Z. A cutting force prediction model, experimental studies, and optimization of cutting parameters for rotary ultrasonic face milling of C/SiC composites. Applied Composite Materials, 2020, 27(4): 407–431
138. Liang Y H, Chen Y, Chen B B, Fan B P, Yan C R, Fu Y C. Feasibility of ultrasonic vibration assisted grinding for carbon fiber reinforced polymer with monolayer brazed grinding tools. International Journal of Precision Engineering and Manufacturing, 2019, 20(7): 1083–1094
139. Li H, Lin B, Wan S M, Wang Y, Zhang X F. An experimental investigation on ultrasonic vibration-assisted grinding of SiO_{2f}/SiO_2 composites. Materials and Manufacturing Processes, 2016, 31(7): 887–895
140. Wang D P, Lu S X, Xu D, Zhang Y L. Research on material removal mechanism of C/SiC composites in ultrasound vibration-assisted grinding. Materials, 2020, 13(8): 1918
141. Wang H, Zhang D Z, Li Y Z, Cong W L. The effects of elliptical ultrasonic vibration in surface machining of CFRP composites using rotary ultrasonic machining. The International Journal of Advanced Manufacturing Technology, 2020, 106(11–12): 5527–5538
142. Azarhoushang B, Tawakoli T. Development of a novel ultrasonic unit for grinding of ceramic matrix composites. The International Journal of Advanced Manufacturing Technology, 2011, 57(9–12): 945
143. Chen T, Li H B, Ye M L, Xiang C, Tian S L. Experimental study on effects of structural characteristics of C/E composite laminates on grinding temperature. Composites Part B: Engineering, 2019, 157: 100–108
144. Liang Y H, Chen Y, Zhu Y J, Ji J J, Ding W F. Investigations on tool clogging and surface integrity in ultrasonic vibration-assisted slot grinding of unidirectional CFRP. The International Journal of Advanced Manufacturing Technology, 2021, 112(5): 1557–1570
145. Wang H J, Sun J, Li J F, Lu L X, Li N. Evaluation of cutting force and cutting temperature in milling carbon fiber-reinforced polymer composites. The International Journal of Advanced Manufacturing Technology, 2016, 82(9–12): 1517–1525
146. Wang F B, Bin Z, Wang Y Q. Milling force of quartz fiber-reinforced polyimide composite based on cryogenic cooling. The International Journal of Advanced Manufacturing Technology, 2019, 104(5–8): 2363–2375
147. Liu M Z, Li C H, Zhang Y B, An Q L, Yang M, Gao T, Mao C, Liu B, Cao H J, Xu X F, Said Z, Debnath S, Jamil M, Ali H M, Sharma S. Cryogenic minimum quantity lubrication machining: from mechanism to application. Frontiers of Mechanical Engineering, 2021, 16(4): 649–697
148. Liu M Z, Li C H, Cao H J, Zhang S, Chen Y, Liu B, Zhang N Q, Zhou Z M. Research progress and application of cryogenic minimum quantity lubrication machining technology. China Mechanical Engineering, 2022, 33(5): 529–550 (in Chinese)
149. Wang X M, Zhang J C, Wang X P, Zhang Y B, Liu B, Luo L, Zhao W, Zhang N Q, Nie X L, Li C H. Effect of nanoparticle volume on grinding performance of titanium alloy in cryogenic air minimum quantity lubrication. Diamond & Abrasives Engineering, 2020, 40(5): 23–29
150. Jia Z Y, Fu R, Wang F J, Qian B W, He C L. Temperature effects in end milling carbon fiber reinforced polymer composites. Polymer Composites, 2018, 39(2): 437–447
151. Zhang B, Du Y, Liu H, Xin L, Yang Y, Li L. Experimental study on high-speed milling of SiC_f/SiC composites with PCD and CVD diamond tools. Materials, 2021, 14(13): 3470
152. Nor Khairusshima M K, Che Hassan C H, Jaharah A G, Amin A K M, Md Idriss A N. Effect of chilled air on tool wear and workpiece quality during milling of carbon fibre-reinforced plastic. Wear, 2013, 302(1–2): 1113–1123
153. Nor Khairusshima M K, Sharifah I S S. Study on tool wear during milling CFRP under dry and chilled air machining. Procedia Engineering, 2017, 184: 506–517
154. Danish M, Gupta M K, Rubaiee S, Ahmed A, Mahfouz A, Jamil M. Machinability investigations on CFRP composites: a comparison between sustainable cooling conditions. The International Journal of Advanced Manufacturing Technology, 2021, 114(11–12): 3201–3216
155. Zou F, Zhong B F, Zhang H, An Q L, Chen M. Machinability and surface quality during milling CFRP laminates under dry and supercritical CO_2-based cryogenic conditions. International Journal of Precision Engineering and Manufacturing—Green Technology, 2022, 9(3): 765–781

156. Zou F, Dang J Q, Wang X F, Zhang H Z, Sun X F, An Q L, Chen M. Performance and mechanism evaluation during milling of CFRP laminates under cryogenic-based conditions. Composite Structures, 2021, 277: 114578
157. Muhamad Khairussaleh N K, Che Haron C H, Ghani J A. Study on wear mechanism of solid carbide cutting tool in milling CFRP. Journal of Materials Research, 2016, 31(13): 1893–1899
158. Morkavuk S, Köklü U, Bağcı M, Gemi L. Cryogenic machining of carbon fiber reinforced plastic (CFRP) composites and the effects of cryogenic treatment on tensile properties: a comparative study. Composites Part B: Engineering, 2018, 147: 1–11
159. Ohashi K, Maeno H, Fujihara R, Kubota S, Yoshikawa M, Tsukamoto S. Influence of grinding atmosphere on grinding characteristics of CFRP (effect of soluble coolant or liquid nitrogen supply). Transactions of the Japan Society of Mechanical Engineers Series C, 2013, 79(808): 5068–5078
160. Fujihara R, Ohashi K, Yoshikawa M, Kubota S, Onishi T, Tsukamoto S. Investigation of grinding temperature of carbon fiber reinforced plastics. In: Proceedings of International Conference on Leading Edge Manufacturing in 21st Century: LEM21, 2013, 103–106
161. Wang F B, Wang Y Q. Effect of fiber orientation on the milling performance of quartz fiber composites in cryogenic cooling. Proceedings of the Institution of Mechanical Engineers, Part C: Journal of Mechanical Engineering Science, 2020, 234(1): 18–31
162. Cococcetta N M, Jahan M P, Schoop J, Ma J F, Pearl D, Hassan M. Post-processing of 3D printed thermoplastic CFRP composites using cryogenic machining. Journal of Manufacturing Processes, 2021, 68: 332–346
163. Larbi S, Bensaada R, Bilek A, Djebali S. Hygrothermal ageing effect on mechanical properties of FRP laminates. AIP Conference Proceedings, 2015, 1653(1): 020066
164. Scida D, Assarar M, Poilâne C, Ayad R. Influence of hygrothermal ageing on the damage mechanisms of flax-fibre reinforced epoxy composite. Composites Part B: Engineering, 2013, 48: 51–58
165. Wu X F, Li C H, Zhou Z M, Nie X L, Chen Y, Zhang Y B, Cao H J, Liu B, Zhang N Q, Said Z, Debnath S, Jamil M, Ali H M, Sharma S. Circulating purification of cutting fluid: an overview. The International Journal of Advanced Manufacturing Technology, 2021, 117(9–10): 2565–2600
166. Haddad M, Zitoune R, Eyma F, Castanie B. Study of the surface defects and dust generated during trimming of CFRP: influence of tool geometry, machining parameters and cutting speed range. Composites Part A: Applied Science and Manufacturing, 2014, 66: 142–154
167. Tang L Z, Zhang Y B, Li C H, Zhou Z M, Nie X L, Chen Y, Cao H J, Liu B, Zhang N Q, Said Z, Debnath S, Jamil M, Ali H M, Sharma S. Biological stability of water-based cutting fluids: progress and application. Chinese Journal of Mechanical Engineering, 2022, 35(1): 3
168. Senthilkumar M, Prabukarthi A, Krishnaraj V. Machining of CFRP/Ti6Al4V stacks under minimal quantity lubricating condition. Journal of Mechanical Science and Technology, 2018, 32(8): 3787–3796
169. Giasin K, Ayvar-Soberanis S, Hodzic A. Evaluation of cryogenic cooling and minimum quantity lubrication effects on machining GLARE laminates using design of experiments. Journal of Cleaner Production, 2016, 135: 533–548
170. Li B K, Li C H, Zhang Y B, Wang Y G, Jia D Z, Yang M, Zhang N Q, Wu Q D, Han Z G, Sun K. Heat transfer performance of MQL grinding with different nanofluids for Ni-based alloys using vegetable oil. Journal of Cleaner Production, 2017, 154: 1–11
171. Wang Y G, Li C H, Zhang Y B, Yang M, Li B K, Dong L, Wang J. Processing characteristics of vegetable oil-based nanofluid MQL for grinding different workpiece materials. International Journal of Precision Engineering and Manufacturing—Green Technology, 2018, 5(2): 327–339
172. Zhang S, Li J F, Wang Y W. Tool life and cutting forces in end milling Inconel 718 under dry and minimum quantity cooling lubrication cutting conditions. Journal of Cleaner Production, 2012, 32: 81–87
173. Yang M, Li C H, Zhang Y B, Wang Y G, Li B K, Jia D Z, Hou Y L, Li R Z. Research on microscale skull grinding temperature field under different cooling conditions. Applied Thermal Engineering, 2017, 126: 525–537
174. Zhang Y B, Li C H, Jia D Z, Li B K, Wang Y G, Yang M, Hou Y L, Zhang X W. Experimental study on the effect of nanoparticle concentration on the lubricating property of nanofluids for MQL grinding of Ni-based alloy. Journal of Materials Processing Technology, 2016, 232: 100–115
175. Jia D, Zhang N Q, Liu B, Zhou Z M, Wang X M, Zhang Y B, Mao C, Li C H. Particle size distribution characteristics of electrostatic minimum quantity lubrication and grinding surface quality evaluation. Diamond & Abrasives Engineering, 2021, 41(3): 89–95 (in Chinese)
176. Jia D Z, Zhang Y B, Li C H, Yang M, Gao T, Said Z, Sharma S. Lubrication-enhanced mechanisms of titanium alloy grinding using lecithin biolubricant. Tribology International, 2022, 169: 107461
177. Jia D Z, Li C H, Zhang Y B, Zhang D K, Zhang X W. Experimental research on the influence of the jet parameters of minimum quantity lubrication on the lubricating property of Ni-based alloy grinding. The International Journal of Advanced Manufacturing Technology, 2016, 82(1–4): 617–630
178. Jia D Z, Li C H, Zhang Y B, Yang M, Cao H J, Liu B, Zhou Z M. Grinding performance and surface morphology evaluation of titanium alloy using electric traction bio micro lubricant. Journal of Mechanical Engineering, 2022, 58(5): 198–211
179. Wang X M, Zhang J C, Wang X P, Zhang Y B, Luo L, Zhao W, Liu B, Nie X L, Li C H. Temperature field model and verification of titanium alloy grinding under different cooling conditions. China Mechanical Engineering, 2021, 32(5): 572–578, 586
180. Wang X M, Li C H, Zhang Y B, Ding W F, Yang M, Gao T, Cao H J, Xu X F, Wang D Z, Said Z, Debnath S, Jamil M, Ali H M. Vegetable oil-based nanofluid minimum quantity lubrication turning: academic review and perspectives. Journal of Manufacturing Processes, 2020, 59: 76–97
181. Guo S M, Li C H, Zhang Y B, Wang Y G, Li B K, Yang M, Zhang X P, Liu G T. Experimental evaluation of the lubrication performance of mixtures of castor oil with other vegetable oils in MQL grinding of nickel-based alloy. Journal of Cleaner

Production, 2017, 140: 1060–1076

182. Shi Z, Guo S M, Liu H J, Li C H, Zhang Y B, Yang M, Chen Y, Liu B, Zhou Z M, Nie X L. Experimental evaluation of minimum quantity lubrication of biological lubricant on grinding properties of GH4169 nickel-base alloy. Surface Technology, 2021, 50(12): 71–84
183. Yang M, Li C H, Zhang Y B, Jia D Z, Li R Z, Hou Y L, Cao H J. Effect of friction coefficient on chip thickness models in ductile-regime grinding of zirconia ceramics. The International Journal of Advanced Manufacturing Technology, 2019, 102(5–8): 2617–2632
184. Yang M, Li C H, Zhang Y B, Jia D Z, Li R Z, Hou Y L, Cao H J, Wang J. Predictive model for minimum chip thickness and size effect in single diamond grain grinding of zirconia ceramics under different lubricating conditions. Ceramics International, 2019, 45(12): 14908–14920
185. Duan Z J, Li C H, Zhang Y B, Dong L, Bai X F, Yang M, Jia D Z, Li R Z, Cao H J, Xu X F. Milling surface roughness for 7050 aluminum alloy cavity influenced by nozzle position of nanofluid minimum quantity lubrication. Chinese Journal of Aeronautics, 2021, 34(6): 33–53
186. Cococcetta N M, Pearl D, Jahan M P, Ma J F. Investigating surface finish, burr formation, and tool wear during machining of 3D printed carbon fiber reinforced polymer composite. Journal of Manufacturing Processes, 2020, 56: 1304–1316
187. Esmaeili H, Adibi H, Rezaei S M. An efficient strategy for grinding carbon fiber-reinforced silicon carbide composite using minimum quantity lubricant. Ceramics International, 2019, 45(8): 10852–10864
188. Adibi H, Esmaeili H, Rezaei S M. Study on minimum quantity lubrication (MQL) in grinding of carbon fiber-reinforced SiC matrix composites (CMCs). The International Journal of Advanced Manufacturing Technology, 2018, 95(9–12): 3753–3767
189. Pervaiz S, Kannan S, Huo D H, Mamidala R. Ecofriendly inclined drilling of carbon fiber-reinforced polymers (CFRP). The International Journal of Advanced Manufacturing Technology, 2020, 111(7–8): 2127–2153
190. Iskandar Y, Tendolkar A, Attia M H, Hendrick P, Damir A, Diakodimitris C. Flow visualization and characterization for optimized MQL machining of composites. CIRP Annals—Manufacturing Technology, 2014, 63(1): 77–80
191. Helmy M O, El-Hofy M H, El-Hofy H. Effect of cutting fluid delivery method on ultrasonic assisted edge trimming of multidirectional CFRP composites at different machining conditions. Procedia CIRP, 2018, 68: 450–455
192. Li M, Yu T B, Zhang R C, Yang L, Ma Z L, Li B C, Wang X Z, Wang W S, Zhao J. Experimental evaluation of an eco-friendly grinding process combining minimum quantity lubrication and graphene-enhanced plant-oil-based cutting fluid. Journal of Cleaner Production, 2020, 244: 118747
193. Yang M, Li C H, Said Z, Zhang Y B, Li R Z, Debnath S, Ali H M, Gao T, Long Y Z. Semiempirical heat flux model of hard-brittle bone material in ductile microgrinding. Journal of Manufacturing Processes, 2021, 71: 501–514
194. Said Z, Sharma P, Sundar L S, Afzal A, Li C H. Synthesis, stability, thermophysical properties and AI approach for predictive modelling of Fe_3O_4 coated MWCNT hybrid nanofluids. Journal of Molecular Liquids, 2021, 340: 117291
195. Cui X, Li C H, Ding W F, Chen Y, Mao C, Xu X F, Liu B, Wang D Z, Li H N, Zhang Y B, Said Z, Debnath S, Jamil M, Ali H M, Sharma S. Minimum quantity lubrication machining of aeronautical materials using carbon group nanolubricant: from mechanisms to application. Chinese Journal of Aeronautics, 2021 (in press)
196. Zhang Y B, Li H N, Li C H, Huang C Z, Ali H M, Xu X F, Mao C, Ding W F, Cui X, Yang M, Yu T B, Jamil M, Gupta M K, Jia D Z, Said Z. Nano-enhanced biolubricant in sustainable manufacturing: from processability to mechanisms. Friction, 2022, 10(6): 803–841
197. Sui M H, Zhang N Q, Li C H, Wu W T, Zhang Y B, Yang M. Theoretical analysis and experiment on temperature field of nano-fluid micro-lubrication grinding cemented carbide. Manufacturing Technology & Machine Tool, 2020, (3): 85–91 (in Chinese)
198. Said Z, Arora S, Farooq S, Sundar L S, Li C H, Allouhi A. Recent advances on improved optical, thermal, and radiative characteristics of plasmonic nanofluids: academic insights and perspectives. Solar Energy Materials and Solar Cells, 2022, 236: 111504
199. Zhang Y B, Li C H, Jia D Z, Zhang D K, Zhang X W. Experimental evaluation of the lubrication performance of MoS_2/CNT nanofluid for minimal quantity lubrication in Ni-based alloy grinding. International Journal of Machine Tools and Manufacture, 2015, 99: 19–33
200. Zhang X P, Li C H, Zhang Y B, Wang Y G, Li B K, Yang M, Guo S M, Liu G T, Zhang N Q. Lubricating property of MQL grinding of Al_2O_3/SiC mixed nanofluid with different particle sizes and microtopography analysis by cross-correlation. Precision Engineering, 2017, 47: 532–545
201. Dong L, Li C, Bai X, Zhai M, Qi Q, Yin Q, Lv X, Li L. Analysis of the cooling performance of Ti-6Al-4V in minimum quantity lubricant milling with different nanoparticles. The International Journal of Advanced Manufacturing Technology, 2019, 103(5−8): 2197–2206
202. Bai X, Li C, Dong L, Yin Q. Experimental evaluation of the lubrication performances of different nanofluids for minimum quantity lubrication (MQL) in milling Ti-6Al-4V. The International Journal of Advanced Manufacturing Technology, 2019, 101(9–12): 2621–2632
203. Yang M, Li C H, Luo L, Li R Z, Long Y Z. Predictive model of convective heat transfer coefficient in bone micro-grinding using nanofluid aerosol cooling. International Communications in Heat and Mass Transfer, 2021, 125: 105317
204. Cui X, Li C H, Zhang Y B, Jia D Z, Zhao Y J, Li R Z, Cao H J. Tribological properties under the grinding wheel and workpiece interface by using graphene nanofluid lubricant. The International Journal of Advanced Manufacturing Technology, 2019, 104(9–12): 3943–3958
205. Gao T, Li C H, Zhang Y B, Yang M, Jia D Z, Jin T, Hou Y L, Li R Z. Dispersing mechanism and tribological performance of vegetable oil-based CNT nanofluids with different surfactants. Tribology International, 2019, 131: 51–63

206. Zhang Z C, Sui M H, Li C H, Zhou Z M, Liu B, Chen Y, Said Z, Debnath S, Sharma S. Residual stress of grinding cemented carbide using MoS_2 nano-lubricant. The International Journal of Advanced Manufacturing Technology, 2022, 119(9–10): 5671–5685
207. Gao T, Li C H, Jia D Z, Zhang Y B, Yang M, Wang X M, Cao H J, Li R Z, Ali H M, Xu X F. Surface morphology assessment of CFRP transverse grinding using CNT nanofluid minimum quantity lubrication. Journal of Cleaner Production, 2020, 277: 123328
208. Gao T, Li C H, Yang M, Zhang Y B, Jia D Z, Ding W F, Debnath S, Yu T B, Said Z, Wang J. Mechanics analysis and predictive force models for the single-diamond grain grinding of carbon fiber reinforced polymers using CNT nano-lubricant. Journal of Materials Processing Technology, 2021, 290: 116976
209. Gao T, Zhang Y B, Li C H, Wang Y Q, An Q L, Liu B, Said Z, Sharma S. Grindability of carbon fiber reinforced polymer using CNT biological lubricant. Scientific Reports, 2021, 11(1): 22535
210. James S, Nejadian S M. Experimental study on high-speed saw cutting of hybrid composite stacks using nanoparticle-enhanced minimum quantity lubrication. The International Journal of Advanced Manufacturing Technology, 2020, 110(11–12): 3077–3090
211. Rodriguez R L, Lopes J C, Mancini S D, de Ângelo Sanchez L E, de Almeida Varasquim F M F, Volpato R S, de Mello H J, de Aguiar P R, Bianchi E C. Contribution for minimization the usage of cutting fluids in CFRP grinding. The International Journal of Advanced Manufacturing Technology, 2019, 103(1–4): 487–497
212. Wang X M, Li C H, Zhang Y B, Said Z, Debnath S, Sharma S, Yang M, Gao T. Influence of texture shape and arrangement on nanofluid minimum quantity lubrication turning. The International Journal of Advanced Manufacturing Technology, 2022, 119(1–2): 631–646
213. Wang F J, Yan J B, Zhao M, Wang D, Wang X N, Hao J X. Surface damage reduction of dry milling carbon fiber reinforced plastic/polymer using left–right edge milling tool. Journal of Reinforced Plastics and Composites, 2020, 39(11–12): 409–421
214. López de Lacalle N, Lamikiz A, Campa F J, Valdivielso A F, Etxeberria I. Design and test of a multitooth tool for CFRP milling. Journal of Composite Materials, 2009, 43(26): 3275–3290
215. Chen Y D, Guo X H, Zhang K D, Guo D L, Zhou C C, Gai L W. Study on the surface quality of CFRP machined by micro-textured milling tools. Journal of Manufacturing Processes, 2019, 37: 114–123
216. Shyha I, Huo D H, Hesamikojidi P, Eldessouky H, El-Sayed M A. Performance of a new hybrid cutting-abrasive tool for the machining of fibre reinforced polymer composites. The International Journal of Advanced Manufacturing Technology, 2021, 112(3–4): 1101–1113
217. Sasahara H, Kikuma T, Koyasu R, Yao Y. Surface grinding of carbon fiber reinforced plastic (CFRP) with an internal coolant supplied through grinding wheel. Precision Engineering, 2014, 38(4): 775–782
218. Yuan H P, Gao H, Liang Y D. Fabrication of a new-type electroplated wheel with controlled abrasive cluster and its application in dry grinding of CFRP. International Journal of Abrasive Technology, 2010, 3(4): 299–315
219. Okuyama S, Kitajima T, Yui A. Grinding performance of a grain-arranged diamond wheel and a GC wheel against CFRP. Journal of the Japan Society for Abrasive Technology, 2011, 55(10): 611–615
220. Handa D, Sooraj V S. An eccentric sleeve grinding strategy for fibre-reinforced composites. Composites Part B: Engineering, 2019, 176: 107332